UTILIZING ACTIVATED PYROLYTIC BIOCHAR AS A CATALYST FOR PYRLOYSIS OF PLASTICS

By

Sara Saeed

(00000275955)

Supervisor: Dr. Muhammad Zeeshan Ali Khan

Institute of Environmental Sciences and Engineering (IESE)

School of Civil & Environmental Engineering (SCEE)

National University of Sciences and Technology (NUST)

Islamabad, Pakistan

2022

Utilizing Activated Pyrolytic Biochar as a catalyst for Pyrolysis of Plastics

By

Sara Saeed

Regn Number

00000275955

A thesis submitted in partial fulfillment of the requirements for the degree of

Masters of Science

in

Environmental Engineering

Institute of Environmental Sciences and Engineering (IESE)

School of Civil & Environmental Engineering (SCEE)

National University of Sciences and Technology (NUST)

Islamabad, Pakistan

2022

Approval Certificate

Certified that the contents and form of the thesis entitled **"Utilizing Activated Pyrolytic Biochar as a catalyst for Pyrolysis of Plastics"** submitted by Ms. Sara Saeed has been found satisfactory for partial fulfilment of the requirements of the degree of Master of Science in Environmental Engineering.

Supervisor: _____

Dr. Muhammad Zeeshan Ali Khan

Associate Professor

IESE, SCEE, NUST

GEC Member: _____

Dr. Zeshan

Assistant Professor

IESE, SCEE, NUST

GEC Member: _____

Dr. Waqas Qamar Zaman

Assistant Professor

IESE, SCEE, NUST

Acceptance Certificate

Certified that final copy of MS/MPhill thesis written by Ms. Sara Saeed (Registration No.00000275955) of **IESE (SCEE)** has been verified by undersigned, found complete in all respects as per NUST Statutes/Regulations, is free of plagiarism, errors and mistakes and is accepted as partial fulfilment for award of MS/ MPhil degree. It is further certified that necessary amendments as pointed out by GEC members of the scholar have also been incorporated in the said thesis.

Signature: _____

Name of Supervisor: _____

Date: _____

Signature (HOD): _____

Date: _____

Signature (Dean/Principal): _____

Date: _____

Declaration Certificate

I certify that this research work titled *"Utilizing Activated Pyrolytic Biochar as a catalyst for the Pyrolysis of Plastics"* is my own work. The work has not been presented elsewhere for assessment. The material that has been used from other sources as been properly acknowledged/referred.

Sara Saeed

00000275955

Plagiarism Certificate

I certify that this research work titled "*Utilizing Activated Pyrolytic Biochar as a catalyst for the Pyrolysis of Plastics"* is my own work. Thesis has significant new work/knowledge as compared to already published or under consideration to be published elsewhere. No sentence, equation, diagram, table, paragraph or section has been copied verbatim from previous work unless it is placed under quotation marks and duly referenced. The thesis has been checked using TURNITIN and found within limits as per HEC plagiarism Policy and instructions issued from time to time.

Sara Saeed Signature: _____

00000275955 Supervisor: _____

Date: _____

Dedicated to my beloved family,

for their tremendous support throughout my research work!

Acknowledgments

I am greatly indebted to Allah Almighty, the beneficent and merciful, whose blessings enabled me to complete this research work in a best manner. I would never able to be at this stage without His will.

"My Lord, indeed I am, for whatever good You would send down to me, in need."
28:24

Firstly, I would like to thank my supervisor Dr. Zeeshan Ali Khan for his constant support, guidance and help throughout my research work, principally he allowed me a room to work in my own way. I am thankful to the guidance offered by my Guidance and Examination Committee members Dr. Zeshan and Dr. Waqas Qamar Zaman. Moreover, I would like to thank Dr. Sara Qaisar (National Centre for Physics, Islamabad) for helping us in getting analysis done. I am highly thankful to IESE labs staff for their cooperation.

I take immense pride in expressing my deepest gratitude to my parents, as none of this would have happened if it was not for their love, support and above all patience. Most importantly, I would like to thank the chief member of my family, my ***Baba*** who has been my backbone and played a significant role in making me what I am today and was always there throughout the challenging phases of my research work.

I appreciate the assistance of my colleagues from NICE as they helped me in a lot of external matters and had been always just one call away.

Last but not the least, I owe a big thanks to my sister like friends ***Mominah Ahmad*** and ***Iqra Naseem*** who have always stood by me and backed me up for the completion of this degree by making me feel confident.

Sara Saeed

Table of Contents

List of Abbreviations

Coconut Shell	**CS**
Activated Carbon	**AC**
Coconut Shell Biochar	**CSBC**
Synthesized Activated Carbon	**SAC**
Commercial Activated Carbon	**CAC**
Polystyrene	**PS**
Brunauer, Emmett and Teller	**BET**
Thermogravimetric analysis	**TGA**
X Ray Diffraction	**XRD**
Scanning Electron Microscopy	**SEM**
High Heating Value	**HHV**
Gas Chromatography-Mass Spectroscopy	**GC-MS**
National Institute of Standards and Technology	**NIST**
Catalyst to Feedstock ratio	**CFR**
Mono aromatic Hydrocarbons	**MAH**
Poly-aromatic Hydrocarbons	**PAH**
Low Density Polyethylene	**LDPE**
High Density Polyethylene	**HDPE**
Fourier Transform Infrared	**FTIR**

List of Tables

List of Figures

Abstract

With the increasing amount of waste plastics being used domestically and industrially, the disposition of those being not reusable is a challenging task. Herein, the production of value-added hydrocarbon through thermal and catalytic pyrolysis of polystyrene (PS) with various biomass-based catalyst like coconut shell biochar (CSBC), synthesized activated carbon (SAC) and commercial activated carbon (CAC) was studied in a fixed bed reactor at 500℃ at catalyst to feedstock ratio (CFR) of 1:1. The SAC has been synthesised by chemical treatment of CSBC with H_3PO_4 and its subsequent thermal treatment in an inert environment. The catalysts were characterized by means of N_2 sorption analysis (specific surface area, pore-volume, average pore width), Fourier Transform Infrared (FTIR) spectroscopy, X-Ray Diffraction (XRD) and Scanning Electron Microscope (SEM) imaging. The characterization of catalysts revealed that CSBC, SAC and CAC have surface areas of 112 m^2/g, 311 m^2/g, and 805 m^2/g while their carbon content is 79.24 wt.%, 84.31 wt.% and 85.21 wt.% respectively. The impact of catalysts on the bio-oil composition from the catalytic and non-catalytic pyrolysis of PS was evaluated. The highest bio-oil yield of 73 wt. % and mono aromatic hydrocarbons (MAH) content of 80.39 peak area % was calculated in thermal pyrolysis of PS. With regards to monoaromatic selectivity, maximum selectivity of Benzene, Toluene, Ethylbenzene and Xylene (BTEX) was noticed when SAC was used as a catalyst. While CSBC and CAC promoted production of aliphatic compounds. Moreover, highest calorific value of 46.14 MJ/kg has been observed in PS/SAC combination which is comparable to that of gasoline

CHAPTER 1

1. INTRODUCTION

During the past two decades the risk and reality of environmental degradation have become more apparent. Growing evidence of environmental problems is due to a combination of several factors since the environmental impact of human activities has grown dramatically because of the sheer increase of world population, consumption, industrial activity, etc. Achieving solutions to environmental problems that we face today requires long-term potential actions for sustainable development. In this regard, renewable energy resources appear to be the one of the most efficient and effective solutions. That is why there is an intimate connection between renewable energy and sustainable development (Murdock, Gibb et al. 2021).

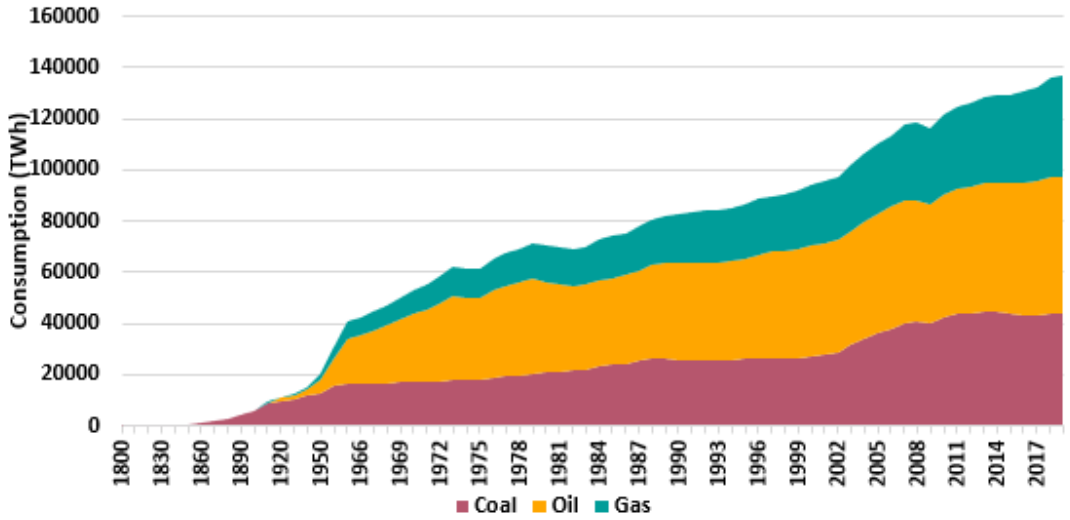

Figure 1.1 Consumption patterns of fossil fuels over last two decades

Rapid industrialization has resulted in maximized use of fossil fuels such as oil, coal and gas. Over the last two decades, the consumption of these fuels has increased manifold. As a result, just 50.8, 50.7 and 114 years of known reserves are left,

worldwide. Excessive use has resulted in global warming, air pollution and water pollution. The patterns of consumption of fossil fuels over the last two decades has been shown in Figure 1.1.

1.1 Energy Mix of the World

The energy mix of the world, presented as total final consumption of primary energy, is displayed in figure 1.2. Comparing the energy mixes of 2009 and 2019, we see that use of fossil fuels has not changed a bit. Among renewables, hydropower dominates followed by biomass, solar and wind whilst biofuels as of yet are only being used in transport sector, majorly. Among renewables biomass being fourth largest source has great potential to be utilized as an energy resource in various applications.

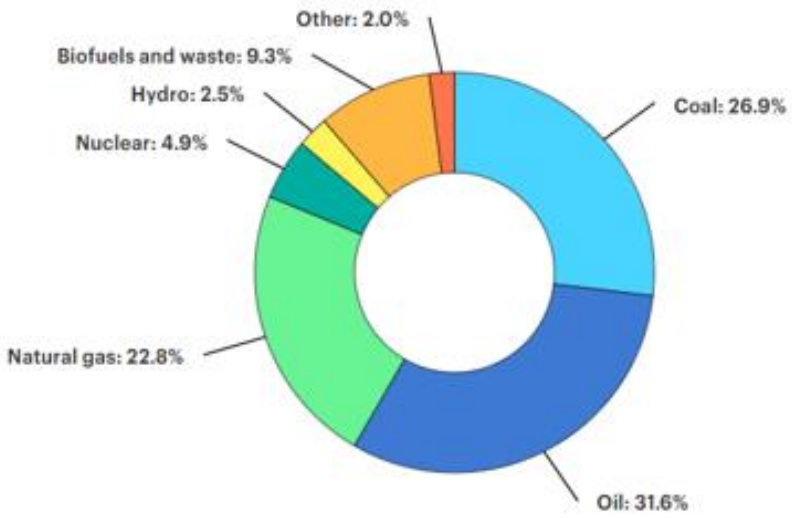

Figure 1.2 Global share of total energy supply over the last decade

1.2 Renewable Energy Sources

Renewable energies are energy sources that are continually replenished by nature and derived directly from the sun (such as thermal, photochemical, and photo-electric), indirectly from the sun (such as wind, hydropower, and photosynthetic energy stored in biomass), or from other natural movements and mechanisms of the environment

(such as geothermal and tidal energy). Renewable energy does not include energy resources derived from fossil fuels, waste products from fossil sources, or waste products from inorganic sources. Renewable energy technologies turn these natural energy sources into usable forms of energy—electricity, heat, and fuels. Figure 1.3 shows an overview of different renewable and non-renewable energy sources (Murdock, Gibb et al. 2021).

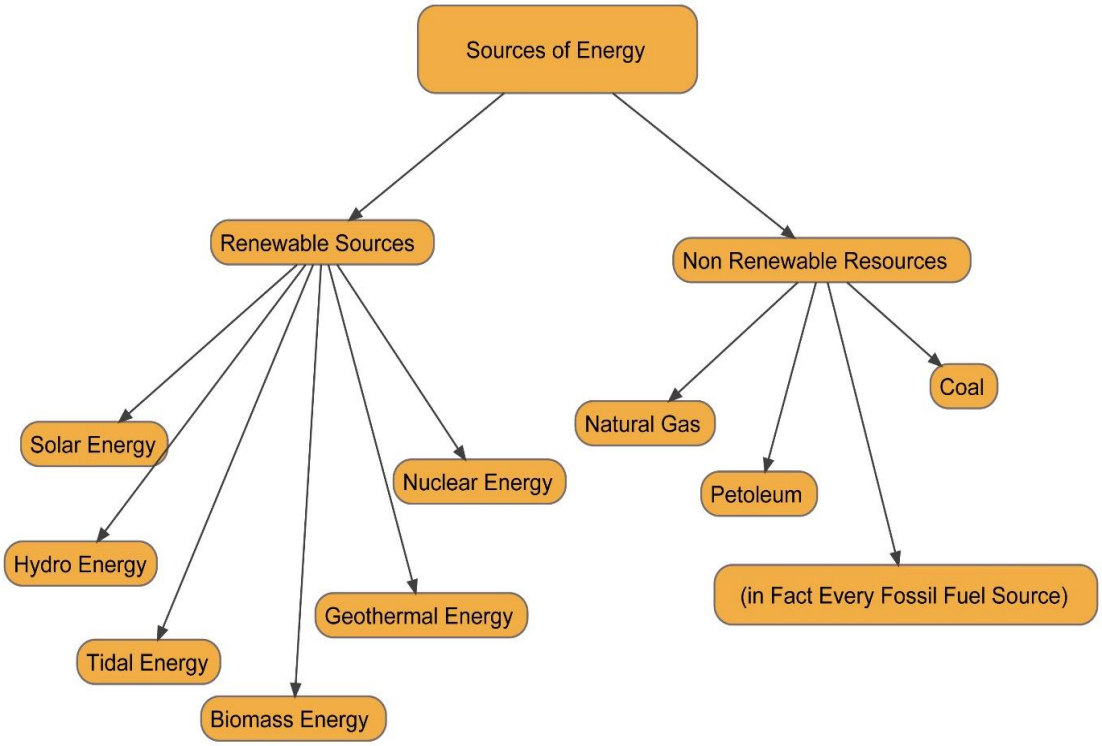

Figure 1.3 Overview of different energy sources

1.3 Plastic Waste Generation and Mishandling

The ever-increasing plastic waste handling is critical issue for the concerned authorities. Currently, the global waste plastic generation stands at 381 million tons per year which is causing serious environmental problems due to its inadequate management. It has been reported that 55% of the of total plastic waste is discarded into the open environment while 26% is subjected to uncontrolled incineration contributing to the air

pollution and climate change (Jambeck, Geyer et al. 2015). Share of plastic waste inadequately managed includes open dumping with little to no recycling are elaborately presented in Figure 1.4. Pakistan is on verge of huge plastic catastrophe as 86% of waste is openly dumped. The menace of inadequate waste management and its consequences, caused by poor planning and management, are aggravating in developing

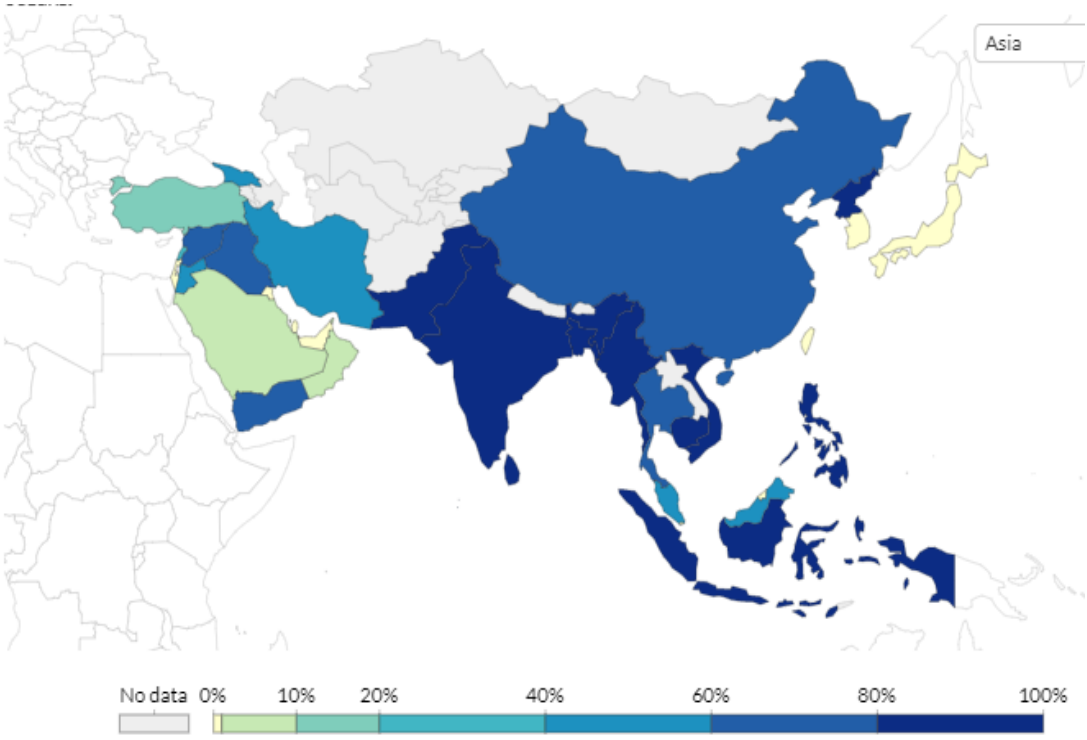

Figure 1.4 Share of plastic waste inadequately managed in Asia

Countries of South Asia and Sub-Saharan Africa (Banu, Sharmila et al. 2020). Conventionally, landfilling, incineration and recycling are the widely employed approaches for solid waste handling. The landfilling of waste plastic requires humongous land space rendering this approach economical unviable. Besides, leakage of the gases could lead to nuisance and degradation of local air quality. Recycling of waste plastic can potentially transform the waste material into useful products and conserve the new resources like raw material and energy besides reducing the waste for land filling. However, mechanical stability and resource recovery is reduced after each

cycle. Additionally, the physical disposal approaches of waste plastic cannot exploit its ultimate potential. On the other hand, incineration of such waste spews harmful criteria pollutants into atmosphere (Yao and Wang 2020). The plastic waste is also recalcitrant to chemical and biological processes and therefore it requires investigation of alternative approaches to harness tits full potential.

Maximum production of plastic waste i.e., upto 60% ends up in landfill resulting in shrinkage of landfill space along with loss of potential hydrocarbons fuel source. Currently, the global research fraternity is widely investigating the valorisation of waste plastic through two different energy recovery technologies namely anaerobic digestion, transesterification, pyrolysis and gasification (figure 1.5). Nonetheless, pyrolysis has superiority over all others approaches due to numerous technical and economic advantages. The pyrolysis can transform the variety of feedstocks into three types of products such as oil, char and gas compared to gasification which focuses on only gas production (Celik, Kennedy et al. 2019). Additionally, the transportation of oil and char is more economical and convenient compared to gases. 10% of the total plastic waste consists of PS that ends up mostly in the landfills as it is difficult to recycle. Moreover, PS possess high energy content of 37.2 MJ/kg, due to which it can be used in energy conversion processes. The valorisation of PS through pyrolysis could be a favourable approach to produce a substitute for liquid fuels and valuable chemicals (Zhao, Korey et al. 2022).

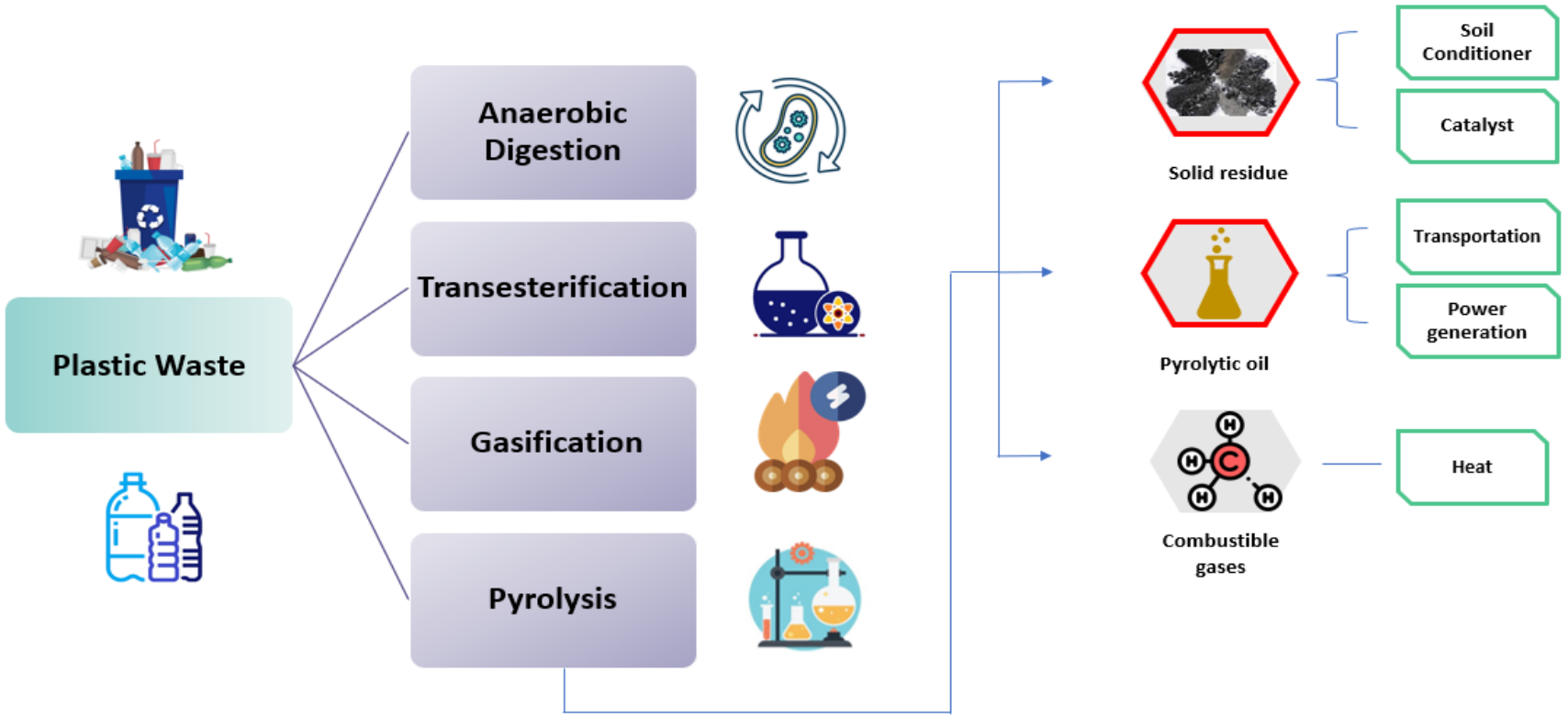

Figure 1.5 Schematic illustration of energy recovery technologies for plastic waste

1.4 Problem Statement

For the upgradation of pyrolytic oil, the use of catalyst having high acidity can be considered. The catalysts promote catalytic activity by following different chemical reactions in the pyrolysis process. However, many unwanted chemical compounds can be generated by this process for which the properties of catalysts needed to be understand thoroughly. Moreover, the price and long-term stability of catalysts must be kept controlled for specific applications during the whole process. Among acidic catalysts, commercial zeolites have shown an excellent catalytic activity in the pyrolysis and co-pyrolysis of waste plastics as well as biomass, by following the various cracking reactions. Different kinds of zeolites such as (ZSM-5 and HZSM-5) have shown better performance in the upgradation of pyrolytic / bio-oil. However, due to limitations of pore size of zeolites structure, many large molecules of pyrolytic oil failed to access the active site of these catalysts. Moreover, the microporosity of zeolites results in its degeneration and formation of coke occurred on the active sites resulting in the deactivation of catalysts. To date, degeneration and deactivation are the main problems that have let the trend, shift towards the use of renewable catalysts. carbon-based catalyst could be the alternative to synthetic and expensive zeolitic catalysts. Now a days, green, cheap and renewable catalysts derived from the biomass waste are found to be effective for the pyrolysis of waste plastics. Among which carbon-based catalysts such as biochar and activated carbon has been found to be more effective catalysts / support materials as they have good ability to improve the quality of pyrolytic oil. The. The use of carbon-based catalysts has been the focus of researchers for application in pyrolysis of plastics due to low costs and higher availability.

1.5 Research Objectives

The objectives of the research work carried out are:

1. Preparation of activated carbon by pyrolytic char.
2. Investigating utility of biochar and activated carbon as pyrolytic catalyst.

CHAPTER 2

2. LITERATURE REVIEW

2.1 Pyrolysis

Pyrolysis is a tertiary recycling technique in which thermal degradation of waste products (normally organic polymers) occurred that results in the formation of small volatile and semi volatile molecules i.e., char, gases and liquid oil. It is the reliable, flexible and conservational technique that supplements increased energy demand from petroleum industries. The formation of small molecules occurred when the vapours at high temperature passed through a condensing unit. This process operates at elevated temperatures of 400 ℃-1000 °C in an anoxic environment. However, for decomposition of plastics, typical temperature range is 500 ℃–550 ℃ (Maqsood, Dai et al. 2021). Liquid oil for broilers, generators and furnaces can be obtained by thermal cracking of waste plastics. Polymers such as polystyrene (PS), polyethylene terephthalate (PET) and poly methyl methacrylate (PMA) can be depolymerized to obtain monomers as they contain different functional groups that favours depolymerization. Three main degradation mechanisms are followed in the pyrolysis namely side scission, side group scission and monomer reversion. Pyrolysis is different from incineration where waste is burnt openly which can produce carcinogenic oxides when volatiles react with oxygen.

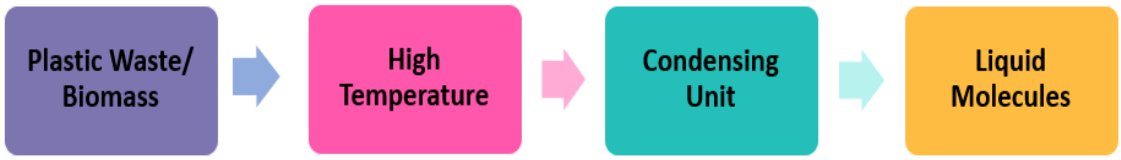

Figure 2.1 Steps in pyrolysis process

2.2 Pyrolysis Products

Pyrolysis of waste material can produce three types of products namely liquid oil which is called pyrolytic or bio oil depending upon the nature of feedstock, solid residue which is called char or biochar and pyrolytic gas.

2.2.1 Pyrolytic Oil

Pyrolytic oil, a product of interest from pyrolysis, is a dark brown organic liquid. It is called bio-oil if the feedstock used in the pyrolysis, is a biomass. Bio oil is mainly composed of oxygenated compounds which lead to the instability and low heating value, resulting in an unusable product for engine fuel.

Pyrolytic oil obtained from plastic waste can result in the pyrolytic oil yield of up to 95 wt.%, with the kinematic viscosity (up to 2.96 mm^2/s), density (0.8 kg/m^3), flash point (~30 °C), cloud point (−18 °C), and high heating value (41.58 MJ/kg). these physicochemical properties are closed to diesel. Approximately 300 ~ 400 distinct chemical compounds of varying molecular weight can generate via thermal and catalytic pyrolysis of plastic waste. Moreover, with the passage of time, the viscosity of pyrolytic oil can increase due to various chemical and physical reactions that result in the aging of the liquid. To avoid the secondary reactions, the pyrolytic oil must be placed at cooled places. Different parameters of pyrolysis such as heating rate, residence time, temperature of pyrolysis, and flow rate of inert gas can improve the efficiency of the quality and quantity of pyrolytic liquid. Furthermore, the particle size of feedstock, type of reactor also play an important role in the products of pyrolysis.

2.2.2 Pyrolytic Gas

Pyrolytic gas is the combination of various hydrocarbons C_xH_y maximum carbon number C_6 and hydrogen gas. In case of biomass, carbon dioxide CO_2, and carbon

monoxide CO can also be produced by the degradation of carboxyl and carbonyl groups during the process. Pyrolytic gas has high potential to be used in the power sector due to its composition as mentioned before and a high net calorific value. The yield and composition of pyrolytic gas varies significantly by the change in reaction temperature. Thermal degradation of feedstock is directly proportional to the increase in reaction temperature. The pyrolysis of plastics produces large number of gases as compared to biomass. For instance, the gas yield during the pyrolysis of PVC and PET was noted to be 87.7 wt.% and 76.9 wt.% which is greater as compared to the yield of gases produced by the pyrolysis of PS. The gas produced by the pyrolysis of PP and PE have high calorific values of 42 - 45 MJ/kg. Thus, this high potential of gas can be used on industrial scales. The pyrolytic gas can also be used in turbines and boilers to produce electricity in power sector.

2.2.3 Solid Residue

Solid residue also called pyrolytic char is the remaining solid product of pyrolysis which is rich in carbon. It is also called biochar if it is the product of biomass, a feedstock that is used for pyrolysis. Pyrolytic char has different physical and chemical properties depending upon the type of feedstock composition and varying pyrolysis conditions. For example, its carbon content could differ from 53 wt.% to 96 wt.%. Furthermore, the yield and heating value of pyrolytic char can also vary in a wide range (30 wt.% - 90 wt.% and 20-36 MJ/kg, separately) that results in a wide range difference of surface area and elemental content.

Char can be used for soil amendment, catalytic activities, energy storage and environmental protection and a sustainable platform carbon material for other high-value applications. A few researchers also used char as an adsorbent for removing impurities from water (Ahmad, Rajapaksha et al. 2014).

The physical properties of pyrolytic char can be varied depending upon different parameters. Among all the factors, temperature being one of the important factors to cause appreciable changes in the structure of char. For instance, at temperature below than 400 ℃ the porous structure of char didn't change much. However, at temperature range between 400 ℃ – 500 ℃ the change in surface area is prominent and it goes on increasing at higher temperature of 900 ℃. This change in surface area is due to the formation of microporous structure that is directly proportional to increase in pyrolysis temperature. The difference in temperature of eucalyptus can be observed in table 2.1 at different temperatures (Hu and Gholizadeh 2019).

Table 2.1 Change in surface area of eucalyptus at various temperatures

Temperature (℃)	**Surface Area (m^2/g)**	**Micropore Volume (mm^3/g)**
600	528	206
700	539	218
800	570	224
900	589	226

2.5 Classification of Pyrolysis based on Operating Conditions

Pyrolysis can be categorized in three main types depending upon the heating rates and residence time of vapours in the reactor. (Table 2.2)

1. Slow pyrolysis
2. Fast pyrolysis
3. Flash pyrolysis

2.5.1 Slow Pyrolysis

The temperature range in slow pyrolysis varies between 300 ℃ to 700 ℃ and the particle size that is preferable for slow pyrolysis is 5 mm – 50 mm. Slow pyrolysis is normally recommended for solid residue production.

2.5.2 Fast Pyrolysis

The fast pyrolysis takes place at heating rate greater than 10 – 200 ℃ /sec and the residence time equals to 0.5 – 10 sec.

2.5.3 Flash Pyrolysis

In flash pyrolysis, the heating rate of 10^3 - 10^4 ℃ /sec and residence time is less than 0.5 sec is used.

Table 2.2 Difference in pyrolysis parameters in slow and fast pyrolysis

Pyrolysis Type	**Conditions**		**Solid (wt.%)**	**Liquid (wt.%)**	**Gas (wt.%)**
	Temp (℃)	**Residence Time**			
Slow	~ 400	hrs - days	35	30	35
Fast	~ 500	~ 1 sec	12	75	13

2.6 Types of Pyrolysis Reactors

Different reactors are in use to obtain the desirable end products with efficient heat transfer rates. The most common reactors used for the pyrolysis are batch reactor, fixed bed reactor, fluidized bed reactor, and conical spouted bed reactor.

2.6.1 Batch Reactor

Batch reactor is more efficient with maximum output as compared to other reactors. It does not allow the reactants or products to leave or enter the system. Schematic layout of batch reactor is shown in figure 2.2. However, there are few disadvantages of a batch reactor as it has high labour cost, faces problems in the removal of reactants and products simultaneously etc. Researchers opted to use batch reactors at laboratory level as its design is complex. For catalytic pyrolysis, plastic wastes are mixed with catalyst in the reactor and coke generates as a residue during the process that decreases the efficiency of catalyst used in the process (Li, Li et al. 2016).

2.6.2 Fixed Bed Reactor

Fix-beds reactor is customary and common, which is effortless and simplest to deal with (Lu, Yoshikawa et al. 2018). In these types of reactors, the feedstock or solid catalysts loaded and packed on the bed of the reactors from where reactants can be converted into products. the designing of the reactor is easy as compared to other types however, due to their irregular shape, problems can be faced while loading a feedstock in the reactor. Feeding of plastics with high viscosities and low thermal conductivities are difficult to deal with in fixed bed reactors. Contrarily, many researchers have chosen he fixed bed reactors including different varieties such as one stage fixed bed and two stage fixed bed reactors, for the pyrolysis of plastics. However, the amount of feedstock differs from milligram to kilogram, which has good application at the research centre

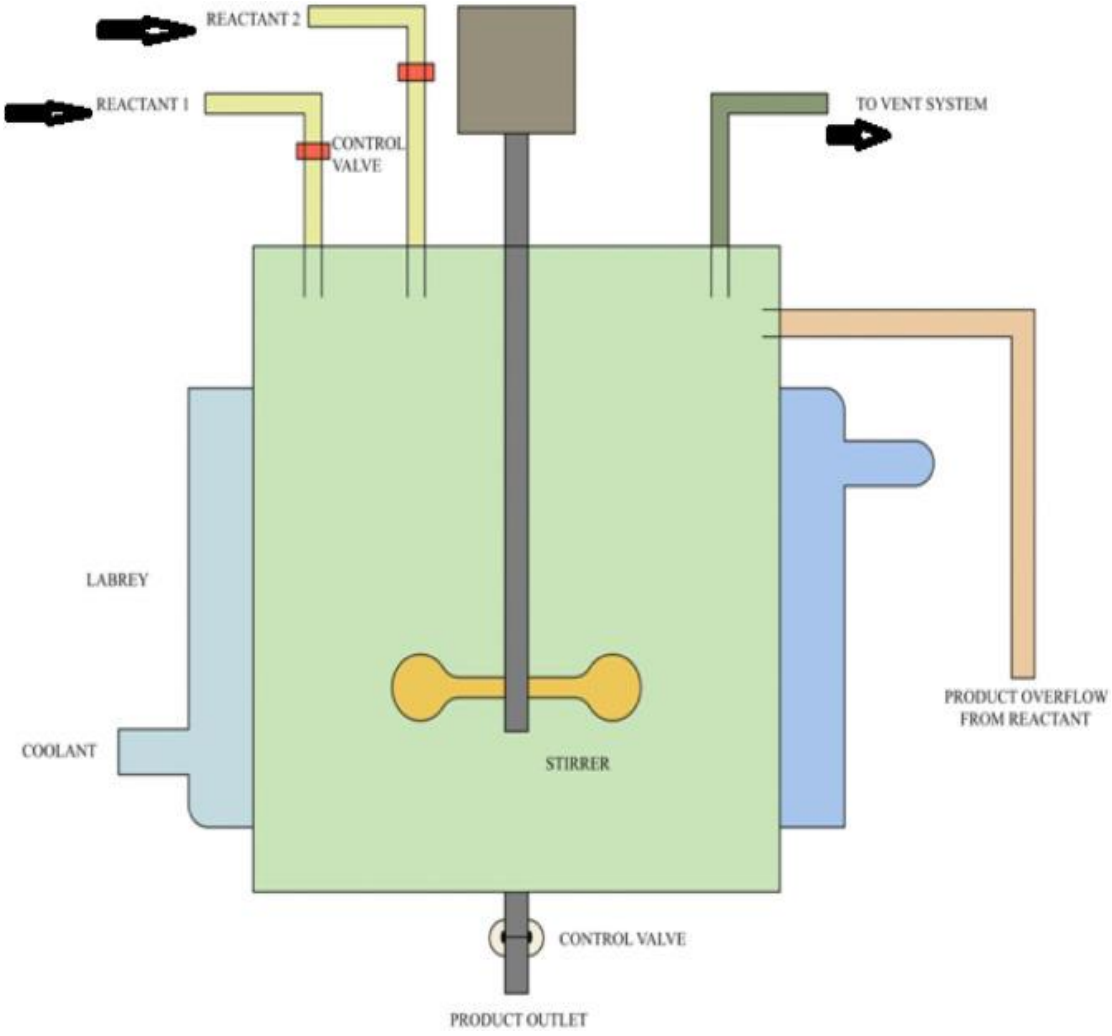

Figure 2.2 Schematic layout of batch reactor

scale. Likewise, it gives sufficient contact between a reactant and a catalyst to effortlessly test the catalytic exhibition. Notwithstanding, it faces the poor heat transfer rates when the scale is broadened (Renzini, Sedran et al. 2009, Lopez, Artetxe et al. 2017). Figure 2.3 shows the layout of fixed bed reactor.

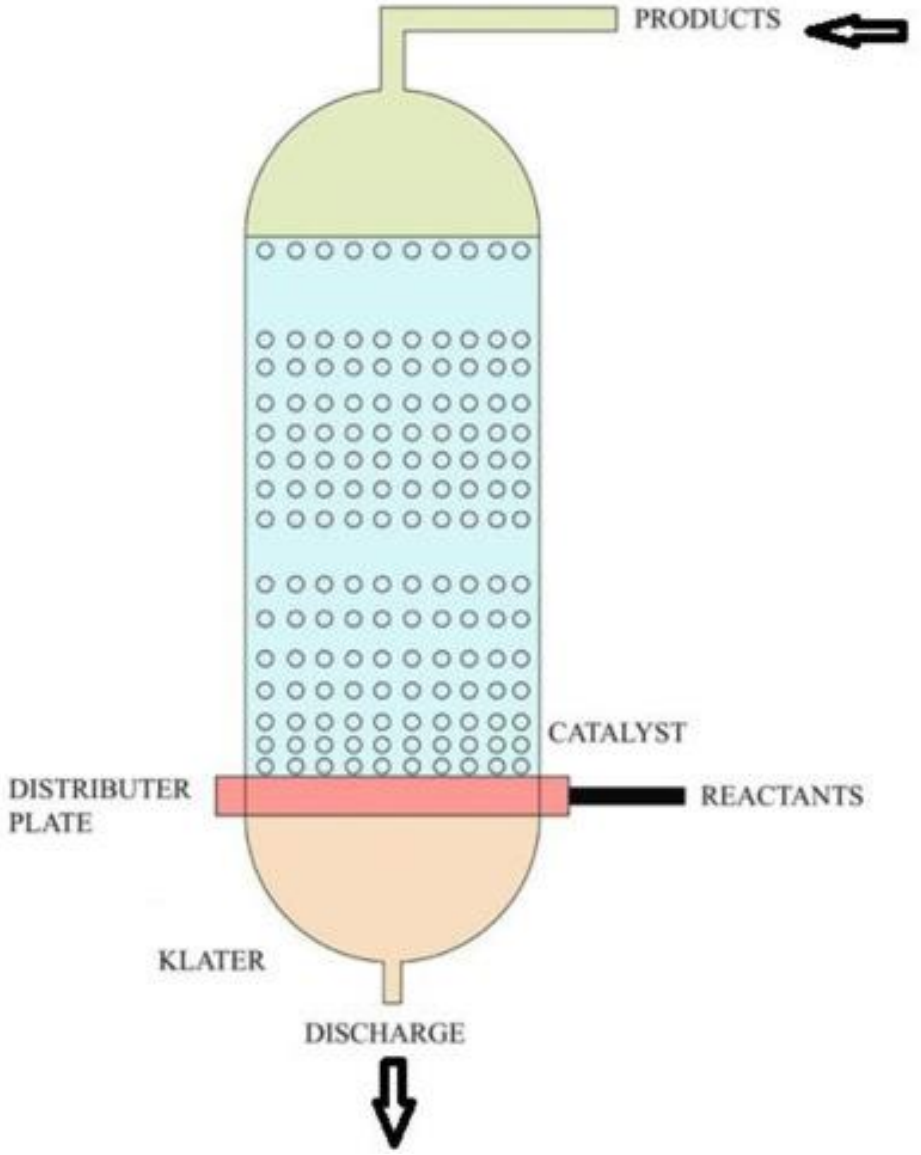

Figure 2.3 Schematic layout of fixed bed reactor

2.6.3 Fluidized Bed Reactor

Fluidized bed reactors have high intensity and mass exchange rates, which pursues it a suitable approach for industrial scale. In these types of reactors, the fluid is usually gas that helps in maintaining the suspension of particles by the high and uniform flowrate of gas. The feedstock or catalyst is loaded on a distributor plate from where the fluidized gas is allowed to pass. The particle size of the feedstock used in the fluidized bed reactor

is much smaller as compared to the fixed bed reactor. the one distinctive advantage that makes the fluid bed reactor superior to other types of reactors is its ability to maintain the excellent uniform temperature in the reactor. However, the bed defluidization brought about by the agglomeration of the catalyst covered with intertwined plastic generally occurs if the working conditions past the portrayed states of the fluidized bed (Lin, Huang et al. 2010, Lopez, Artetxe et al. 2018).

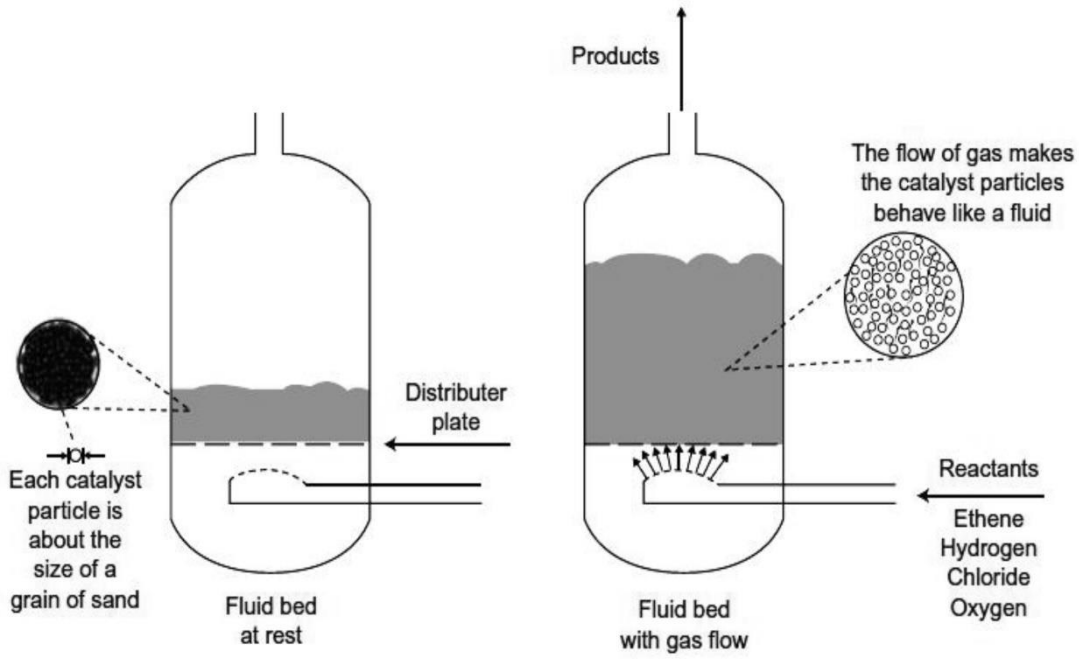

Figure 2.4 Schematic layout of fluid bed reactor

2.6.4 Conical Spouted Bed Reactor

Conical spouted bed reactor is another decision, where high intensity and mass exchange and somewhat slender item dissemination can be accomplished. The design of conical spouted bed reactors is more complex and have high operation cost as compared to fixed and fluidized bed reactors. However, it provides the high heat conductivity rates and better fluid conversion ratios. Conical spouted bed reactor is found to be effective for adhesive materials as the amount of wax decreases linearly

with the increase in temperature, after several researchers explored the catalytic pyrolysis of low density and high-density polyethylene at various temperatures. yet issues of increasing and restrictions on bed material particles actually exist (Elordi, Olazar et al. 2011).

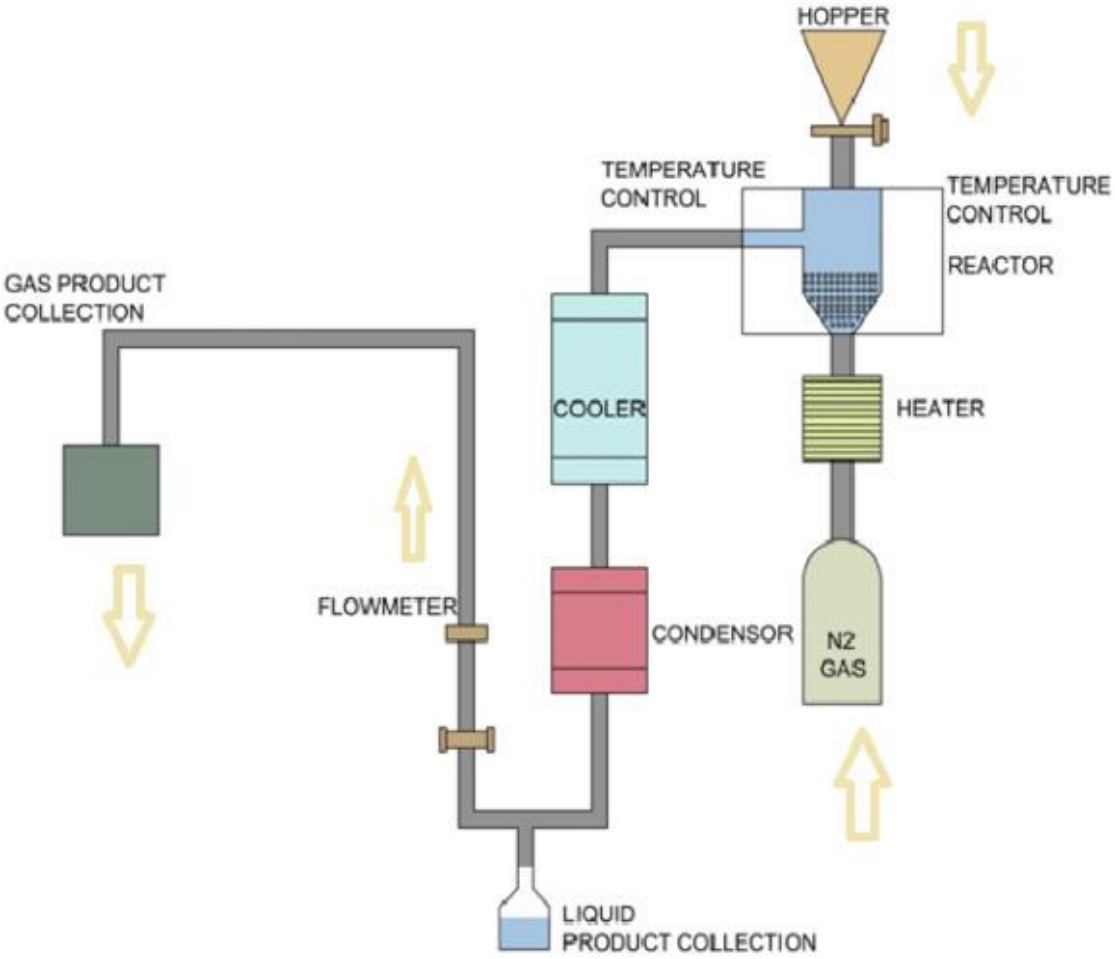

Figure 2.5 Schematic layout of conical spouted bed reactor

2.7 Types of Pyrolysis

Pyrolysis process can be classified as thermal or catalytic. Thermal pyrolysis is carried out at high temperatures in the absence of catalysts whereas, in catalytic pyrolysis, catalysts are used to enhance the quality of products of pyrolysis mainly liquid oil. The end products of both processes are similar but with different energy outputs (Figure 2.6).

2.7.1 Thermal Pyrolysis

Thermal pyrolysis or non catalytic pyrolysis is an endothermic process that is carried out in the absence of catalyst. Thermal pyrolysis of various plastic types such as PE (LDPE and HDPE), PS and PP has been extensively studied previously. Whereas the literature on the studies of PVC, PET, and poly methyl methacrylate is limited. Thermal

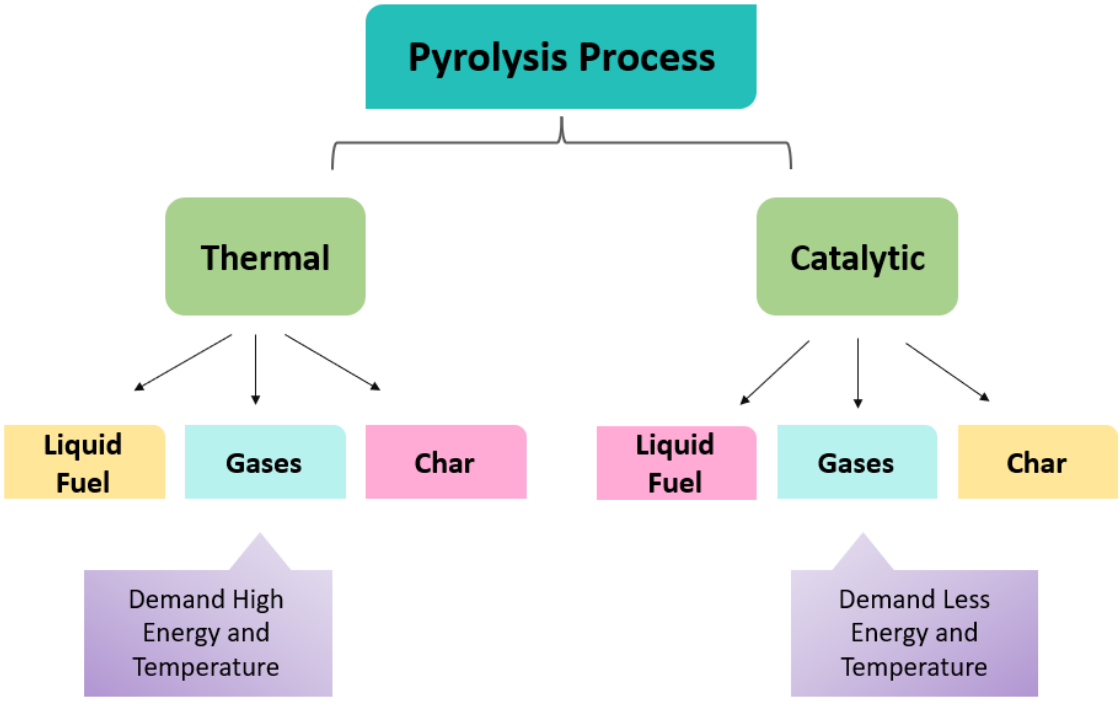

Figure 2.6 Schematic illustration of thermal and catalytic pyrolysis

pyrolysis of PS is easy to carry out as compared to LDPE, HDPE, and PP in the absence of catalyst as it can degenerate completely at the temperature range of 450 ℃ – 500 ℃ higher temperatures. Furthermore, LDPE and HDPE form waxes when thermally decompose without the aid of catalyst. Plastics yield liquid oil containing high carbon chain hydrocarbons with inferior quality when thermally pyrolyzed. However, the percentage yield of liquid oil is greater as compared to the oil yield obtained by catalytic

pyrolysis (Kasar, Sharma et al. 2020). Different roles of all seven types of resins in pyrolysis process have been mentioned below in table 2.3.

Table 2.3 Suitability of different plastics for pyrolysis

Resin Type	Suitability for Pyrolysis	Remarks	References
Polystyrene (PS)	Excellent	• Produce less viscous oil as compared to PP and PE. • Required low energy for conversion into liquid oil.	(Lee and Shin 2007) (Siddiqui and Redhwi 2009)
Polyethylene (LDPE, HDPE)	Very good	• Wax formation occurred in thermal pyrolysis. • Greater than 500 C temperature is required for conversion due its branched chain structure.	(Miskolczi, Angyal et al. 2009) (Lee and Pyrolysis 2012)
Polypropylene (PP)	Very good	• PP is the second most difficult after PE for thermal degradation. • In catalytic pyrolysis, produces high aromatic yield.	(Miskolczi, Angyal et al. 2009)

Polyvinyl chloride (PVC)	Not suitable	• In thermal pyrolysis, hazardous chlorine gas is produced. • In catalytic pyrolysis, presence of chlorine affects the activity of catalyst.	(López, De Marco et al. 2011) (Lopez-Urionabarrenechea, De Marco et al. 2012)
Polyethylene terephthalate (PET)	Not suitable	In thermal pyrolysis, it produces large number of solid fractions.	(Miandad, Barakat et al. 2016)

2.7.2 Catalytic Pyrolysis

Catalytic cracking is one more potential strategy applied to acquire excellent pyrolytic oil because of a few technical benefits. For example, it is performed at environmental strain, it doesn't need water or any other dissolvable, and hydrocarbons (HCs) in the scope of non-renewable energy sources. It can be specifically delivered through different catalysts especially silica alumina catalysts (zeolites). Among all, synthetic zeolites e.g ZSM-5 are the most investigated and viable catalysts studied so far, because of their shape selectivity and textural properties. Acidic sites (Lewis and Bronsted) of zeolitic catalysts, advance polymerization, hydrodeoxygenation, decarbonylation, decarboxylation, hydrocracking, and hydrogenation reactions of different mixtures create desired petroleum products.

2.8 Types of Catalysts

The choice of a catalyst plays a vital role in deciding results from catalytic pyrolysis of waste plastics. Catalysts play a vital role in improving the quality of pyrolysis products as well as lowering the activation temperature and retention time of products. Acid catalysts such as homogenous and heterogenous (figure 2.7) are widely used catalysts and are highly efficient in showing catalytic activity. Despite being economical, they have few disadvantages as they corrode the equipment causing the environmental issues. However, Fe_2O_3, $Ca(OH)_2$, FCC, natural zeolite and synthetic zeolite are some other catalysts that have been explored for their catalytic activity during catalytic pyrolysis process. The utilization of catalysts enhanced the rate of the cracking reactions that lead to an increased yield of pyrolytic gases with a decrease yield of pyrolytic oil (Syamsiro, Saptoadi et al. 2014). Nonetheless, the nature of pyrolytic oil is improved qualitatively, whereas some long chain hydrocarbons are either adsorbed on the surface of catalyst or further broke down into smaller hydrocarbon compounds. Catalyst characteristics, for example, BET surface region, pore size, pore volume, and acidity are the primary factors that influence the catalytic activity of any catalyst in the pyrolysis.

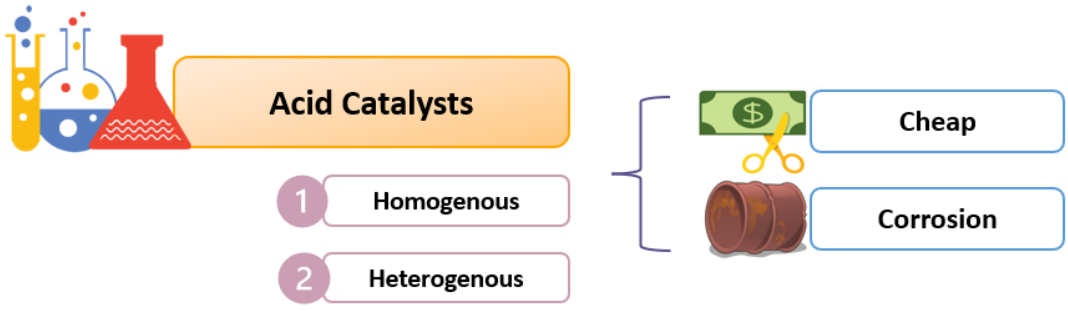

Figure 2.7 Classification of Acid catalysts

2.8.1 Zeolites

Zeolites are aluminosilicates, crystalline in nature forming a regular channel framework that have been widely used as catalysts for catalytic cracking in the catalytic pyrolysis. Zeolites possess varying porosity and Al/Si ratio that promotes the production of aromatics hydrocarbons. These catalysts are mostly acidic in nature as they possess acidic sites (Bronsted vs Lewis acidic sites) on their surface which enhance the generation of aromatic yield by deoxygenation reaction of oxygenates. Zeolites are further divided into two categories namely, natural zeolites and synthetic zeolites as shown in figure 2.8. Natural zeolites are naturally occurring zeolites and found on the outer crust of earth. They have shown a sharp selectivity in the formation of various hydrocarbons and are economical to use. On the other hand, synthetic zeolites that include modified zeolites with metals and metal oxides have been used to enhance the catalytic properties of catalysts in pyrolysis process. The product selectivity is achieved by modifying zeolites with different metals such as Pb, Zn, Ni, Ga, Mo and Co and metal oxides ZnO or MgO respectively. Synthetic zeolites have shown an excellent catalytic performance however, the formation of selective intermediates in the cracking of molecules diffuse into the pore structure of zeolites causing the coke formation on the surface of zeolites that ultimately results in the deactivation of catalyst. Due to limitation of pore size of zeolites, the active sites of the catalyst failed to get access by few of the large components of liquid oil. Therefore, this rapid deactivation of synthetic zeolites will not allow the catalytic activity to proceed further resulting in degeneration of catalyst (Maneechakr and Karnjanakom 2021).

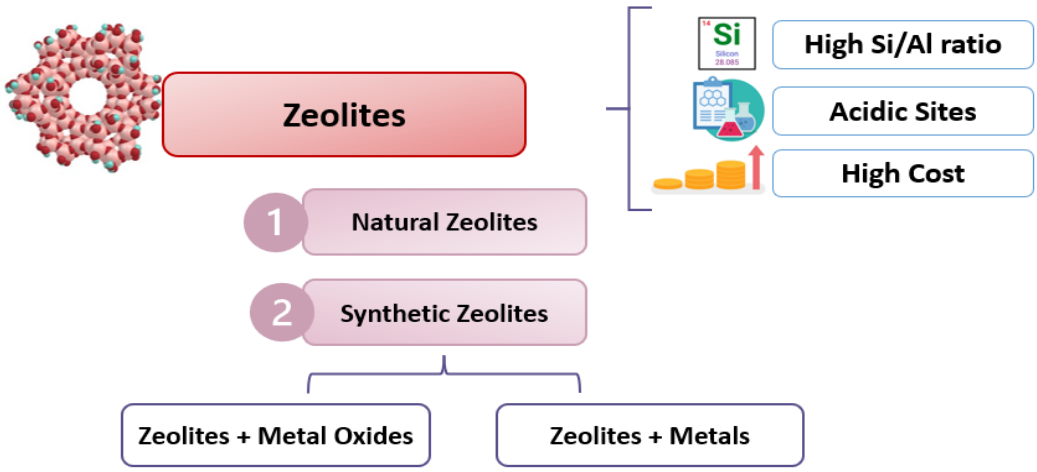

Figure 2.8 Classification of Zeolites

2.8.1.1 Synthetic Zeolites

Synthetic zeolites are accounted for to be promising catalysts for the upgradation of pyrolytic oils nonetheless, their high creation cost might compromise the economics of production and processes at commercial scale. A wide assortment of catalysts has been tested in catalytic pyrolysis of plastics, among which zeolites (for example silica-alumina, β-zeolite, Y-zeolite, HZSM-5, MCM-41) have been confirmed to be observable in creating advanced hydrocarbons lumped in fuel range. These catalysts speed up the carbocation cracking of volatiles, resulting reactions of isomerization, oligomerization, and hydrogen transfer. Analysis of the components resulted from catalytic pyrolysis using synthetic zeolites have shown that the corrosive strength, exceptional surface region, and porosity of a catalyst were conclusive factors on showing high catalytic execution. Moreover, less carbonaceous coke will accumulate on the surface of ZSM-5 catalyst because of the tridimensional porous structure giving way to the aromatic coke precursors toward the surface of zeolite micropores. Catalytic pyrolysis of polyolefins has been explored in the presence of HZSM-5 to get

hydrocarbons made from non-condensable olefins in the range of C1- C4 gases (Miskolczi, Angyal et al. 2009). Also, the remarkable catalytic execution has been achieved effectively in fix bed, spouted bed, fluidized bed, and microwave-assisted reactors, which shows that HZSM-5 is the most suitable catalyst for the development of gasoline range hydrocarbons (Castano, Elordi et al. 2011, Elordi, Olazar et al. 2011). An extra benefit that against the catalyst deactivation further empowers HZSM-5 the capability of use on commercial scale.

2.8.1.2 Natural Zeolite

Natural zeolites (NZ) are richly found on the outer layer of earth with comparable compositional, primary, cracking, and deoxygenation attributes as that of synthetic zeolites. Consequently, these could be conservative choice to yield a range of important synthetic compounds. Natural zeolites having comparable catalytic properties remain to be neglected materials to a great extent, which might actually work on the economy of the cycle for fuel and chemical production. Natural zeolite shows a sharp selectivity in the formation of gasoline ranged hydrocarbons by speeding up isomerization and aromatization reactions attributable to the extraordinary properties of the zeolitic system, counting the corrosive strength, outer surface chemistry, and microporous surface.

2.8.2 Carbon Based Catalysts

To resolve the problems faced by the use of zeolites, the trend have shifted towards carbon based catalysts. Carbon-based catalyst could be the alternative to synthetic and expensive zeolitic catalysts. Now a days, green, cheap and renewable catalysts derived from the biomass waste are found to be effective for the pyrolysis of waste plastics. Among which carbon-based catalysts such as biochar and activated carbon has been

found to be more effective catalysts / support materials as they have good ability to improve the quality of pyrolytic oil. The. The use of carbon-based catalysts has been the focus of researchers for application in pyrolysis of plastics due to low costs and higher availability.

2.8.2.1 Biochar

Biochar is the carbon rich charring content that is obtained from pyrolysis of biomass. The natural carbon rich roasting content created from pyrolyzed biomass is called biochar. It contains rich oxygen content almost 27-34% as phenolic and carboxylic acid functional groups with the presence of sulfonic groups that leads to enhanced catalytic activity and absorption of other molecules on the surface of biochar. Biochar is a profoundly fixed carbon substance obtained from the various organic products remarkable for some applications due to its conspicuous traits, for example, strength, porosity, and CO_2 sequestration (Wijitkosum and Jiwnok 2019). It is almost 65% carbon content and are synthesized by thermal disintegration of biomass under less or no oxygenic conditions (Choudhary, Khan et al. 2019, Wijitkosum and Jiwnok 2019). The charred biomass primarily contains different percent of carbon, hydrogen, nitrogen, sulphur, and oxygen and it differs from biomass to biomass. The physicochemical properties of biochar relies upon i) type of feedstock/biomass used ii) pyrolysis temperature iii) residence time inside the reactor iv) activating methods and agents v) type of reactor (Mukome, Zhang et al. 2013, Jien 2019). Practically a wide range of biochar, beginning from wood waste to agricultural residues have been utilized as soil fertilizers and as catalysts for different applications.

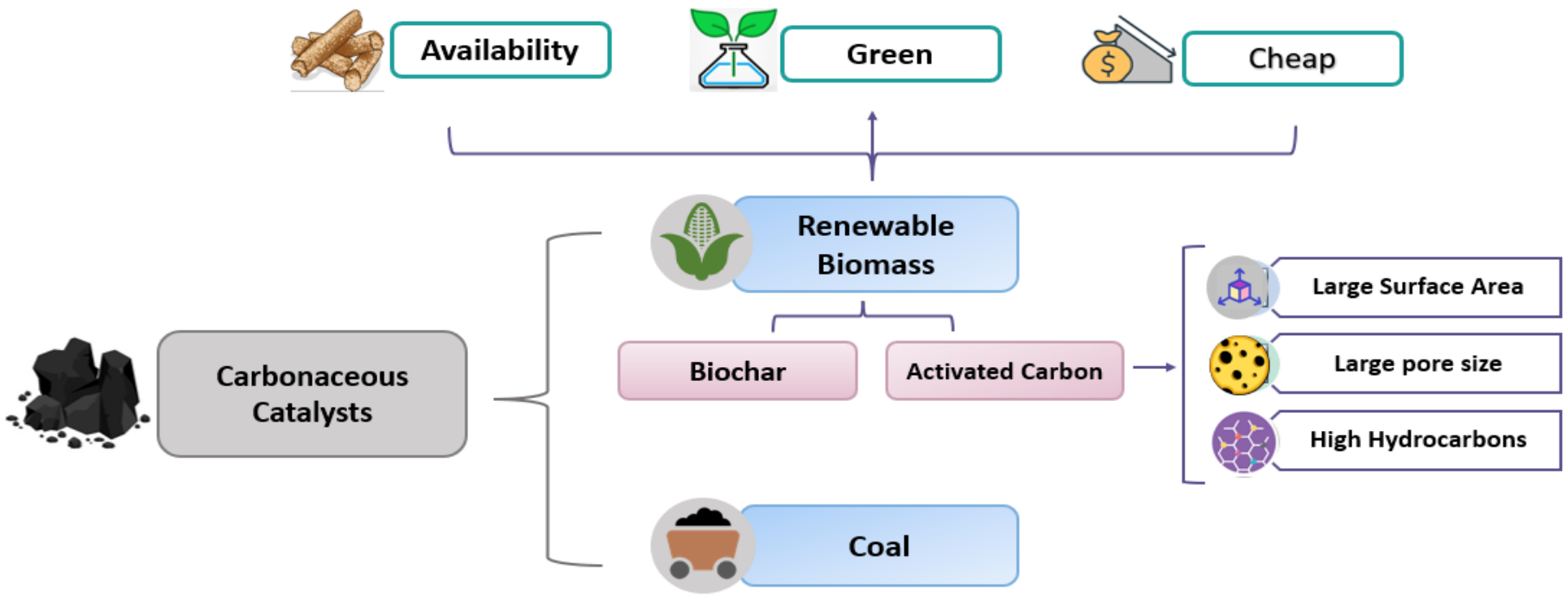

Figure 2.9 Schematic illustration of carbon-based catalysts

A few noticeable changes in soil properties with biochar application have been noticed. It is normally observed that surface area of soil is significantly expanded by use of biochar in light of the fact that it is profoundly microporous in nature (Mukherjee and Lal 2014). Nonetheless, a field preliminary uncovered that use of oak biochar couldn't essentially change surface region of a residue topsoil (surface area of soil: 18 m^2/g) more than a 4-month time span when compared (Mukherjee and Lal 2014). Matured biochar has been accounted for having higher surface region as compared to fresh biochar, and accordingly longer time maintenance and soil biochar microorganisms' interaction are as yet expected to investigate any impact on soil surface region (Zhao, Coles et al. 2015). Maize stover biochar synthesized at 350 °C and 550 °C didn't further develop accessible water capacity when it was applied (11.3 Mg ha^{-1}) to residue topsoil over a span of 295 days, which may be credited to blockage of soil micropores by small parts of applied biochar (for example mineral part or ash). A field experiment (four months) showed that resistance of water permeability in soil was diminished by 10% - 18% when oak biochar pyrolyzed at 650 °C was applied to residue soil. It gave the idea that soil compaction wouldn't be improved by biochar on transient use of application yet maturing of biochar may change soil properties (Mukherjee and Lal 2014).

The biochar can be employed as the most suitable renewable heterogenous catalyst due to following reasons. it is economical due to its cheaper coat, contains large surface area, and presence of various functional groups on its surface. These properties make it an ideal catalyst for the production of bio diesel (Chi, Anto et al. 2021). Biochar has stable structure, high thermal and mechanical stability, chemically inert and it possesses environmentally friendly nature. Biochar is acquired through thermochemical cycles like pyrolysis, HTC, torrefaction, and hydrothermal liquefaction. Temperature, pressure, and biomass synthesis assume an imperative role in the development of

biochar and the biochar yield percentage might change between the thermochemical strategies (Cao, Sun et al. 2017).

2.8.2.2 Activated Carbons

Activated carbons (ACs) that can be obtained from coal as well as renewable biomass stand out on the catalytic pyrolysis of biomass to get value added hydrocarbons due to their large surface area, porosity, and increased acidic sites for the catalytic activity (do Couto Fraga, Quitete et al. 2016, Yang, Lei et al. 2018). Furthermore, the tunable properties can be accomplished by using activated carbons treated with different physical and chemical activation processes. Numerous studies have shown a reasonable connection between the porous structure of a catalyst and the molecular weight of corresponding catalytic products, i.e., large pore size catalysts resulted in higher molecular weight hydrocarbons. Additionally, cracking and aromatization responses were uncovered to rely upon the acidic strength of the catalyst (González-García and Reviews 2018). Enlivened by these, we can assume that ACs can act as appropriate catalysts in acquiring particular hydrocarbons and the jet fuel range hydrocarbons could be created straightforwardly from catalytic pyrolysis of waste plastics.

For AC utilization ion various applications, various precursor materials and preparation methods are used synthesis of AC.

Number of cheap raw materials with high carbon content can be utilized as a precursor materials for the synthesis of activated carbon. The properties of the subsequent activated carbon not only depend upon the type of raw material, but also on the preparation and activation method to be used. Fossil and sustainable sources for the synthesis of activated carbon are mentioned and discussed below.

i. Coal
ii. Wood
iii. Agricultural waste
iv. Ionic liquids and deep eutectic solvents.
v. Precursor solutions

In the start of the 1990s, 360 kilotons activated carbon were delivered, by which 42% is depended on coal as forerunner because of the accessibility and low shore of coals, for example, brown coloured coals, bituminous coals, petrol cokes or anthracites. The coals ought to have a low mineral matter substance and subsequently, low ash content. Bituminous coal-based activated carbons bring about an advanced porous structure because of the presence of primary pores in the coals. This is due to the extremely small size of pores. Activated carbons synthesized from bituminous coals are sturdier contrasted with other coal-based carbons. Petrol coke as result of the treatment facility industry, show a high carbon content, low levels of ash and is easily accessible. Anthracites are truly reasonable antecedents for activated carbon (AC) planning, since they are high-rank coals (high C to H nuclear proportion without carbonization) and show a relevant volume of extremely fine micropores (Yang, Yue et al. 2017).

Non-fossil antecedents for the arrangement of activated carbons are of extraordinary interest because of a rising interest of these materials. Wood and the lignocellulosic polymers from forestry and agriculture are appropriate for this reason. Wood is principally made out of cellulose (40 to 55 wt. %), hemicelluloses (for the most part xylan in hardwoods with 20 to 35 wt. %) and lignin (18 to 35 wt. %). Cellulose keeps up with the construction of the cell walls of plants and is the most bountiful natural substance with a creation of 1011-1012 tons each year, trailed by lignin as second most plentiful unrefined substance (Gupta, Carrott et al. 2016). Lignin is a three-layered

phenolic polymer and is liable for the cementation of cellulose strands in plants. Hemicelluloses, overwhelmingly xylan, are non-cellulosic polysaccharides with a similar low sub-atomic weight. Suhas et al. surveyed the utilization of cellulose as well as lignin for activated carbon arrangement exhaustively (Gupta, Carrott et al. 2016). Hameed and collaborators arranged high surface region AC from wood sawdust (Foo and Hameed 2012).

The utilization of any agricultural waste as raw material for activated carbon materials having high carbon content is of incredible interest. The composition and structure of the used raw material decides the reactivity during pyrolysis and activation steps and in this manner, the subsequent elemental composition. The pyrolysis of lignocellulosic waste gives up to two times the biochar acquired from wood waste. Different beginning materials yield activated carbons with varying content of ash or BET surface regions. Nutshells and cherry stones show for instance less ash content contrasted with grape seeds. Olive stones and bagasse brings about activated carbons with high surface regions, though straw is less appropriate to deliver activated carbons with high surface areas. Yahya et al. referenced that the yields of the activated carbons prepared from these agricultural residues, is lower contrasted with anthracite or coal as beginning materials. Despite this, high volatile matter substance in the biomass is worthwhile for the development of permeable activated carbon materials as well as the minimal expense of the agricultural waste (Yahya, Al-Qodah et al. 2015).

Zhang et al. exhibited the arrangement of carbon materials with high surface regions from protic ionic fluids and salts. The precursors have low-atomic masses, are easily accessible and economical. Synthesis of the carbon materials is straightforward: Neutralization of the nitrogen-containing bases, e.g., phenanthroline or 3-cyanopyridine with sulfuric acid and ensuring removal of the dissolvable prompts the

ideal protic ionic fluids and salts. Carbonization at 1000 °C results in carbon materials with high nitrogen content minus any additional change. The essential parts of the protic ionic fluids impact the yield of the materials. Thermally steady benzene moieties increment essentially how much carbon material delivered, though blends in light of amines or heterocycles decline the yields (Zhang, Miran et al. 2014). The salt templating strategy adopted by Antonietti and collaborators produces carbon materials with high surface regions from ionic fluids. A characterized salt combination was added to the ionic fluids 1-butyl-3-methylpyridinium dicyanamide (Bmp-dca, N-doped materials) or 1-ethyl-3-methylimidazolium tetracyano borate (Emim-tcb, N-and B-doped materials) and the combination was heated in an anoxic environment. Removal of the salt by submerging in water for a few hours, filtration and drying in vacuum prompts the desired carbon material (Fechler, Fellinger et al. 2013). Iwanow et al. examined profound eutectic solvents as unrefined components for activated carbon creation. They broke up the metal salts currently in the low dissolving combinations before pyrolysis and arranged carbon-upheld metal catalysts in one-step. In any case, the overall surface area of these materials is much lower as compared to the conventional and commercial activated carbons, yet high nitrogen contents are achieved relying upon the composition of the profound eutectic solvents (Iwanow, Finkelmeyer et al. 2017).

Xu et al. involved energy-rich carbon antecedents for the circular carbon arrangement through ultrasonic spray pyrolysis. Lithium, sodium, or potassium propiolates are one class of such energy rich materials and possess leaving groups, for example, CO, CO2 or C2H2. Poly (propiolate) salts are framed by polymerization of the initial materials upon heating. The various cations of the propiolates cause changes thermally since various temperatures are expected for the deterioration or various measures of gases are

delivered. Soluble base salts of acetylene dicarboxylic acids can likewise be utilized as precursor for the readiness of carbon spheres. The structure and morphology of the carbon spheres can be affected by the used soluble base salts (Xu, Guo et al. 2012).

Various methods of preparation mfor the activated carbon have been explained further. Different pre-treatment steps according to carbon source, can be adopted for the carbonization/pyrolysis and activation of the raw material. specific techniques i.e., salt templating and ultrasonic spray pyrolysis are introduced along with the most generally utilized strategy for physical or chemical activation. Nevertheless, most important methods are

i. Pre- treatment
ii. De-ashing / demineralization
iii. Physical activation
iv. Chemical activation

Different pre-treatment steps are fundamental before carbonization or activation of the carbonaceous materials. The utilization of biomass as carbon source requires frequently extra washing to eliminate inorganic materials. Drying at 100 °C for a definite interval of time, eliminates the moisture content in the material, which could affect the carbonization process. A specific material size of the precursor for activated carbon is important for the activated carbon preparation process and is achieved by processing and sieving of the carbon materials (Mazlan, Uemura et al. 2016).

Activated carbons contain different ash contents because of presence of inorganic minerals in the raw materials, which influence the chemical properties of the final products. The activated carbons containing lowest ash content can be utilized for catalytic applications. Before production of activated carbons from the raw materials,

ash content and undesirable minerals in the materials are eliminated by using acidic or basic solutions. Samples are generally demineralized by concentrated hydrochloric and hydrofluoric acids as indicated by the Radmacher and Mohr Hauer strategy (Iwanow, Gärtner et al. 2020). The stepwise treatment with hydrochloric acid, hydrofluoric acid and again hydrochloric acid eliminates the metal oxides and silica in the samples. The treatment with HNO3 is one more possibility for de ashing nonetheless, this can cause the oxidation of the material and consequently, generates new oxygen-containing surface functionalities.

Physical activation of carbon materials is a two-step process. After carbonization of the raw materials for a specific time at a requisite temperature under an oxygen free environment steam, air or CO2 activate the materials at higher temperatures (800-1000 °C) to form a porous structure with high surface area (Khuong, Nguyen et al. 2021). The chemical reactions have been mentioned in the equations below.

$$C + O_2 \longrightarrow CO_2 \quad (1)$$

$$C + CO_2 \longrightarrow 2CO \quad (2)$$

$$C + 2H_2O \longrightarrow CO_2 + 2H_2 \quad (3)$$

It is important to take out a high measure of fixed carbon for the development of carbon containing advanced textural properties. Generally, the physical activation of carbon materials is preferred over chemical activation to avoid any sort of impurities or contaminants in the final products from the reaction of activating agents used for activation (Li, Lu et al. 2021).

A few findings show a higher reactivity of steam as gentle oxidizing reagent contrasted with carbon dioxide. However, no reasonable grounds were found in regard to the pore advancement (Zuo, Zhang et al. 2020, Liu, Paskevicius et al. 2021). Rodríguez-Reinoso et al. and Zamora and associates examined the impact of the different physical activation gases on the improvement of porosity from olive stone-based biochar. They inferred that activation with steam brings about activated carbon materials with less micropore volumes and more extensive pore size dispersions (higher volumes of meso- and macropores are shaped) contrasted with carbon dioxide (Román, González et al. 2008). Kalderis et al. arranged activated carbons from bagasse and rice husk by physical and chemical activation. They found that physical activation results in altogether lower surface areas contrasted with the surface areas got by chemical activation with zinc chloride at a similar temperature (Kalderis, Bethanis et al. 2008).

Chemical activation is a one-step technique. Impregnation or blending of the carbon source with the activating agent and ensuing carbonization of that combination prompts exceptionally porous activated carbon materials (Kosheleva, Mitropoulos et al. 2019). The activation agents advance a cross-structure development because of lacking hydration properties, which causes formation of rigid lattice. This construction is less effective to the loss of volatile matter and volume compression during the carbonization bringing about higher activated carbon yields since no carbon burn off is possible. Moreover, additional benefits of the chemical activation are lower temperatures for pyrolysis, the formation of high surface regions and feasibility to control the formation of microporosity, e.g., a thin pore size distribution can be obtained. Furthermore, some other parameters that impact the arrangement of porosity during the chemical activation process for the different preparation conditions are, the selection of the activating agent (KOH, NaOH, $ZnCl_2$, H_3PO_4, $MgCl_2$, $AlCl_3$, K_2CO_3, and so forth), the impregnation

strategy utilized or physically mixing processes, the activation reagent to carbon raw materials ratio, the flowrate of inert gas during carbonization and the pyrolysis temperature and time (Ugwu, Agunwamba et al. 2020).

Numerous chemical reagents have been utilized for activation during the chemical activation process. As per the acid-basic theory and activation mechanism, activating agents can be divided into four categories, i.e., alkaline, acidic, neutral, and self-activating agents. Various kinds of activating agents result in various chemical products when react with cellulose, hemicellulose, lignin, or polysaccharide in carbon precursor, prompting different activation components, which ought to be sorted out for various applications. The porous structure of AC is created through the synergistic impact of pore development, pore extension, pore combination and pore collapse (Gao, Yue et al. 2020).

CHAPTER 3

3. Materials and Methods

3.1 Raw Material

Preparation and characterization of coconut shell has been described in the next sections in detail.

3.1.1 Preparation

Coconut shell (CS) was used as a raw material for the synthesis of catalyst i.e., coconut shell biochar and activated carbon. Raw CS was procured from a local vendor in Rawalpindi, Pakistan as shown in figure 3.1. CS was sundried and chopped into small particles with the help of hammer. Afterwards, the chopped CS pieces were ground through mechanical grinder followed by sieving through sieve no. 16 and 30 to obtain a uniform particle size in the range of 0.6-1.1mm.

Figure 3.1 Raw coconut shell

3.1.2 Characterization

CS was characterized for high heating value (HHV), elemental composition and proximate analysis. HHV of raw material and feedstock was carried out in accordance with the standard method ASTM D5861-1 using Isoperibol oxygen bomb calorimeter.

The ultimate analysis was performed using CHN-S elemental analyser (CKIC 5E-CHN2200) to calculate the elemental composition of CS and PS. Furthermore, for the proximate analysis of raw material and feedstock, standard procedure of ASTM D7291-96 was followed Khan et al. 2021. Thermogravimetric analysis (TGA) of PS and CS was conducted by Mettler Toledo TG analyser. Sample of 6 mg for CS was heated in aluminium oxide crucible from room temperature to the high temperature of 900°C respectively. The TGA experiment was carried out under an inert environment at a ramp rate of 20°C/min. Additionally, Fourier Transform Infrared Spectroscopy (FTIR) analysis in the range of 4000-400cm^{-1} and Scanning Electron Microscopy (SEM) analysis of CS were performed using Bruker FTIR spectrometer (ALPHA II) and (TESCAN VEGA3) respectively (Khan, Zeeshan et al. 2021).

3.2 Feedstock

Polystyrene (PS) was used as a feedstock in the catalytic and non-catalytic pyrolysis. For that PS beads of 1mm (figure 3.2) were purchased from a local petrochemical industry in Rawalpindi, Pakistan and used without any pre-treatments.

Figure 3.2 Polystyrene beads

3.2.1 Characterization

PS was characterized for high heating value (HHV), elemental composition and proximate analysis by the similar standard methods as that of CS mentioned before in section 3.1.2. Thermogravimetric analysis (TGA) of PS was conducted by Mettler Toledo TG analyser. 9 mg of sample for PS was heated in aluminium oxide crucible from room temperature to the high temperature of 900°C respectively. The experiment was carried out under an inert environment at a ramp rate of 20°C/min.

3.3 Catalysts

Three different catalysts have been used in pyrolysis of polystyrene which are as followed:

i. Coconut shell biochar CSBC
ii. Synthesized Activated Carbon SAC
iii. Commercial Activated Carbon CAC

The catalyst was prepared in two phases including (1) carbonisation of CS to obtain CSBC followed by (2) the chemical activation of CSBC to SAC to ensure brevity.

3.3.1 Coconut Shell Biochar

For CSBC production, CS (0.6-1.1mm) was carbonized in a fixed bed reactor, for which slow pyrolysis or conventional carbonization technique was opted. Prior to pyrolysis, CS was dried at 105°C in an oven for 24 hours to make it moisture free. After drying, CS was fed into the reactor and the reactor was closed and purged with nitrogen gas at a flowrate of 500 mL/min for 30 minutes for the provision of inert environment. Thereafter, CS was carbonised at a temperature of 600°C for 2 hours under the constant nitrogen gas flowrate at 100 mL/min to obtain CSBC. It has been reported that biochar

prepared in the temperature range of 400°C to 900°C exhibits high surface area and microporous structure however the properties are superior for biochar prepared in temperature range of 600°C to 900°C (Hu and Gholizadeh 2019). Afterwards, CSBC was ground and strained through sieve no. 80 to obtain a fine powder sample which was preserved in desiccator until its application in pyrolysis reactions.

3.3.2 Synthesized Activated Carbon

Synthesized Activated Carbon has been prepared in two steps.

i. Activation of biochar
ii. Washing of Activated Carbon

For the activation of CSBC, 10 grams sample of powdered CSBC was dissolved in 200 ml of 36% H_3PO_4 solution with solid to liquid ratio of 1/20 adopted from previous literature (Tsang, Hu et al. 2007) (Sun, Huang et al. 2018). The mixture was continuously stirred at room temperature for 2 hours using a magnetic stirrer. Afterwards, the resultant mixture was dried in a microwave oven for 36 hours and was thermally treated at temperature of 650°C in a fixed bed reactor for 2 hours.

Washing of an activated carbon has been done in two steps.

i. Initial washing.
ii. Final washing.

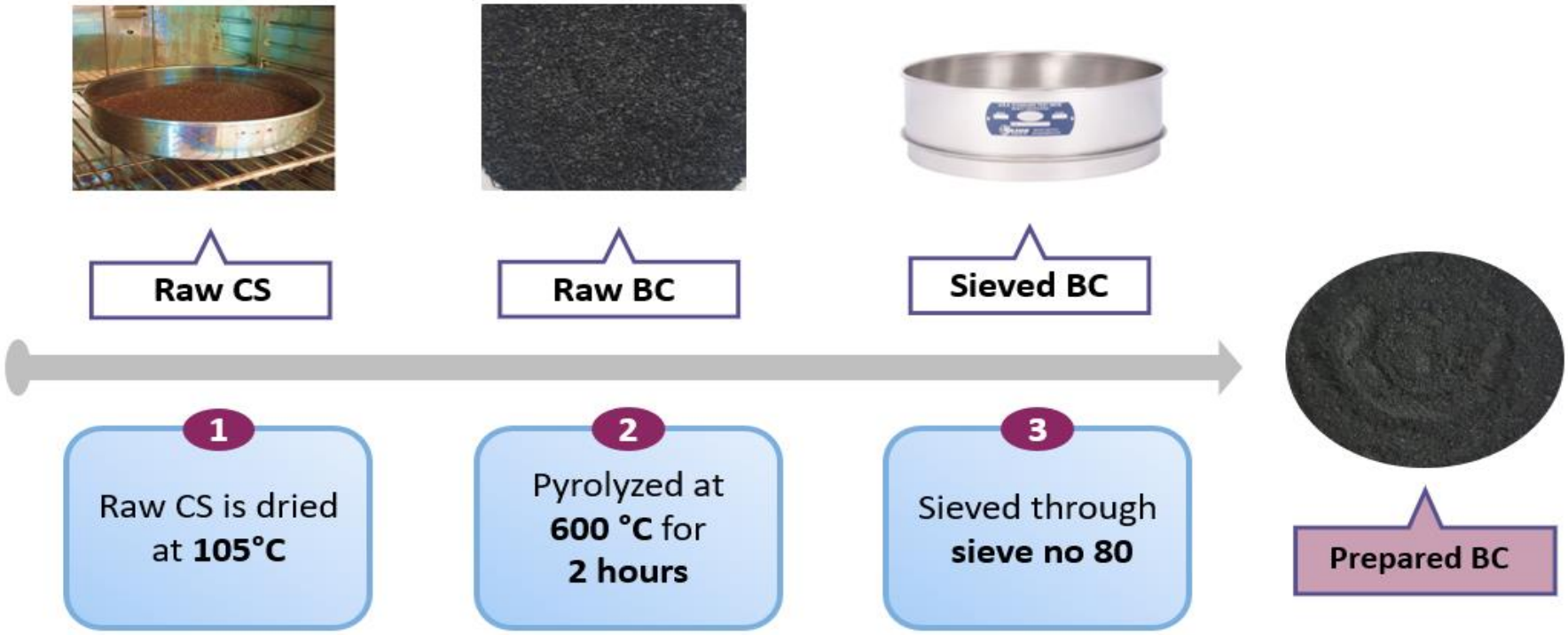

Figure 3.3 Preparation of CSBC

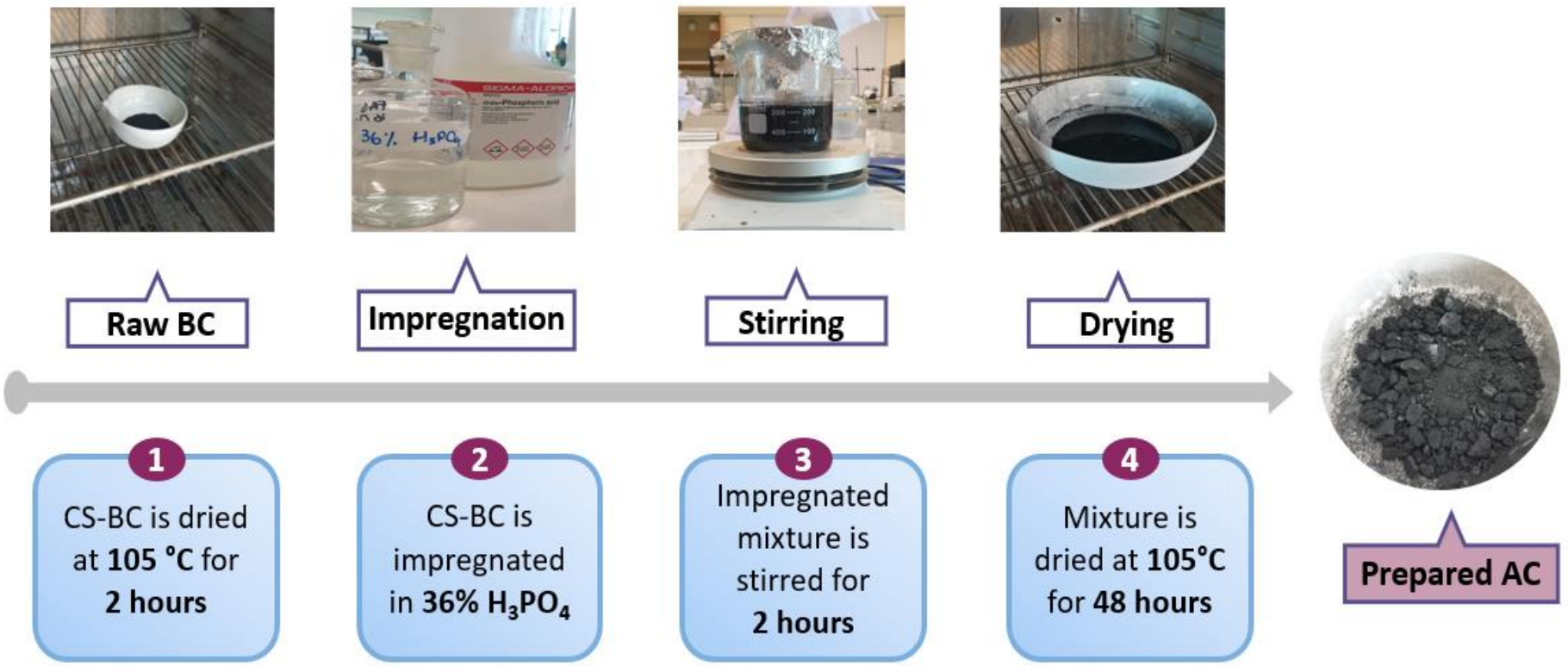

Figure 3.4 Preparation of SAC

Initial washing of self-synthesised activated carbon was done by using acid washing method. In this method hydrochloric acid has been used. 0.1N solution of HCl was prepared by diluting the acidic solution with the help of distilled water. The SAC was then saturated in 0.1N HCl solution. About 20 grams of SS-AC was mixed in a 200mL solution of 0.1N HCl. 500mL beaker was used for this purpose. Afterwards, the solution was kept on a magnetic stirrer and stirred continuously at 200 rpm for 4 hours. The HCl mixture containing SAC was filtered through funnel containing filter paper on it. The residue, which was SAC, was collected from filter paper at the end.

In final washing of SAC, the residue collected after filtration from initial washing was washed with the hot distilled water. The temperature of distilled water was 50°C and SAC was washed 3-4 times until the pH was turned to the neutral. Once the pH of value 7 was achieved, the SAC was collected in a China dish and kept in an oven at 105°C for 36 hours for drying. After the removal of moisture, the SAC was ready to use as a catalyst in the pyrolysis of plastics in a catalytic reactor (Mateo, Lei et al. 2020).

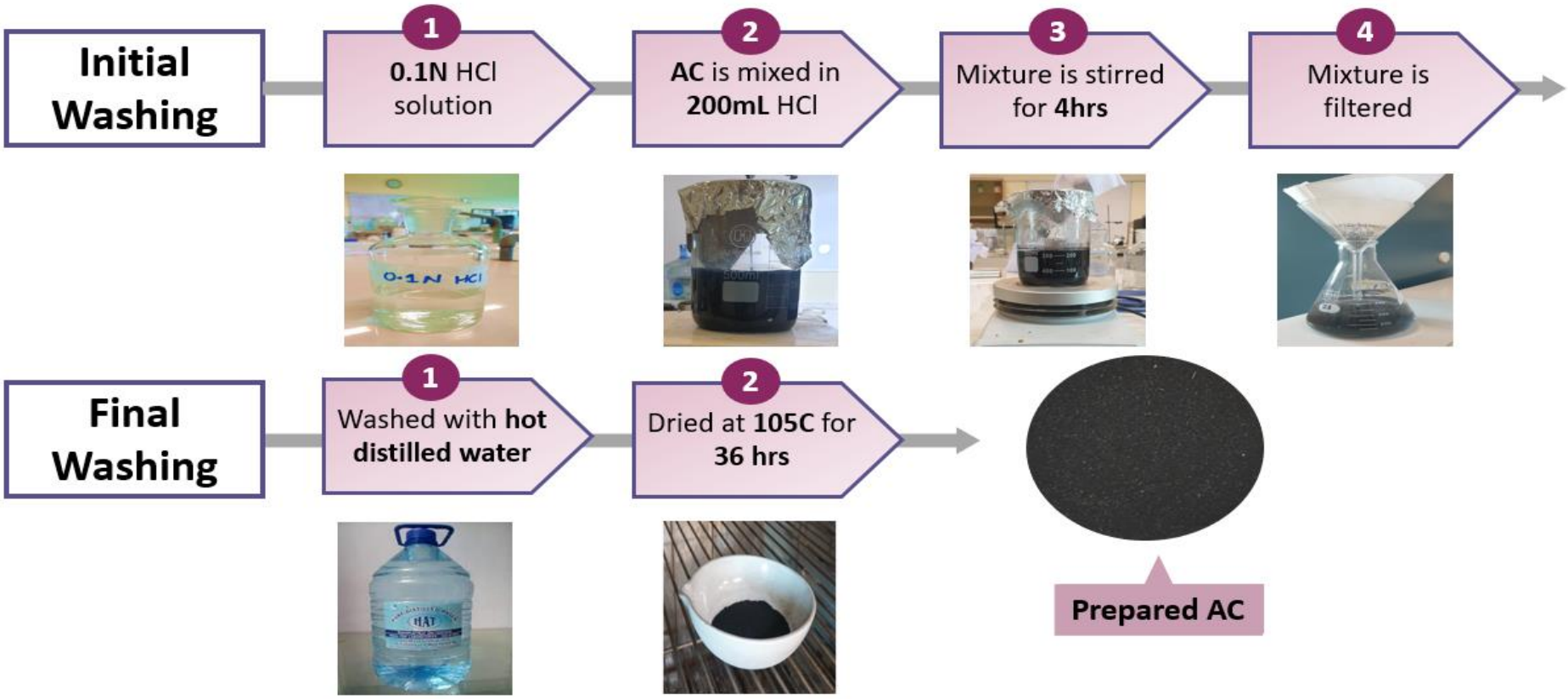

Figure 3.5 Initial and final washing of SAC

3.3.3 Commercial Activated Carbon

Granular commercial activated carbon was purchased from Thailand. It was then finely ground by the aid of mechanical grinder and sieved through sieve no 80. The finely ground commercial activated carbon as shown in figure 8, was dried at 105°C overnight prior to use as a catalyst in the pyrolysis of plastics in a catalytic reactor.

All the three catalysts, CSBC, SAC and CAC, were dried at 105°C for 24 hours prior to various analysis.

Brunauer-Emmet-Teller (BET) method was employed to calculate catalysts textural properties. Surface area, pore size and pore volume of catalysts were analysed by the adsorption of nitrogen gas at 77.3 K using Micrometrics 'Gemini VII 2390 Series of surface area analyser. The catalyst samples were degassed at 5 hours at 200°C in a VacPrep 061-Micrometrics degasser before BET analysis to ensure the removal of air and extraneous material from the pores. To determine the crystalline structure of catalysts, X ray diffraction (XRD) analysis was carried out using X Ray Diffractometer (BRUKER-D8). The catalysts were scanned at a scanning range of $2\Theta = 10°- 90°$ with the scanning speed and step size of 1sec /step and 0.04° respectively. FTIR spectra of all the catalysts were performed in the range of 4000-400cm^{-1} by Bruker FTIR spectrometer (ALPHA II) to determine the presence of functional groups of catalyst. Scanning electron microscopy (SEM) was performed to analyse the surface morphology of catalysts using (TESCAN VEGA3). Prior to analysis, the amorphous samples were converted into conductor by placing them in a sputtering unit. All the images were taken at a resolution of 10 µm and a voltage of 20kV. Moreover, proximate analysis of catalysts was carried out to analyse their fixed carbon, volatile matter, and

ash content through standard method of ASTM D7291-96. The elemental composition of catalysts was assessed using CHN-S elemental analyser (CKIC 5E-CHN2200). To understand the mass degradation of catalysts at high temperatures, thermogravimetric analysis of catalyst samples was performed by Mettler Toledo TG analyser where 8 mg sample was used. The analysis was carried out under an inert nitrogen environment while sample was heated form room temperature to 900°C with the ramp rate of 20°C/min.

3.4 Experimental Setup

In the experimental setup, the type of reactor used for the pyrolysis process that is fix bed reactor and the experimental conditions for the thermal and catalytic pyrolysis of polystyrene has been explained in detail in the following sub sections.

3.4.1 Fixed Bed Reactor

Catalytic pyrolysis experiments are performed in a lab scale fixed bed reactor consisting of two stainless steel cylindrical reactors which are connected vertically through a stainless-steel tube as shown in figure 3.1. The first reactor (R1) was used for the pyrolysis of feedstock and is declared as pyrolysis reactor whereas volatiles produced from decomposition of feedstock in the R1 are passed through catalyst bed in the second reactor (R_2), hence called catalytic reactor. Nitrogen gas (99.99%) was used for the purging of the entire system at a flow rate of 500 mL/min prior to experimentation while flow rate of sweeping gas was maintained at 100 mL/min during experimental run. It was introduced from the bottom of the R1. Ceramic band heaters, controlled by K-type thermocouple and PID, were used around both reactors to provide heat required for pyrolysis reaction in R1 and catalyst activation and cracking reactions in R2. Additionally, both reactors were insulated with the ceramic wool and fibre cloth to

enhance the heating efficiency. A custom-made condenser consisting of copper tube, having ice-salt (NaCl) mixture to maintain the low temperature (-5°C), was connected at downstream of R_2. The catalyst was sandwiched between the layer of ceramic wool adjacent to steel mesh while loading in R2, to avoid the possible sweeping of the powdered catalyst into the condenser pipe which might cause blocking of condenser pipe resulting in backpressure.

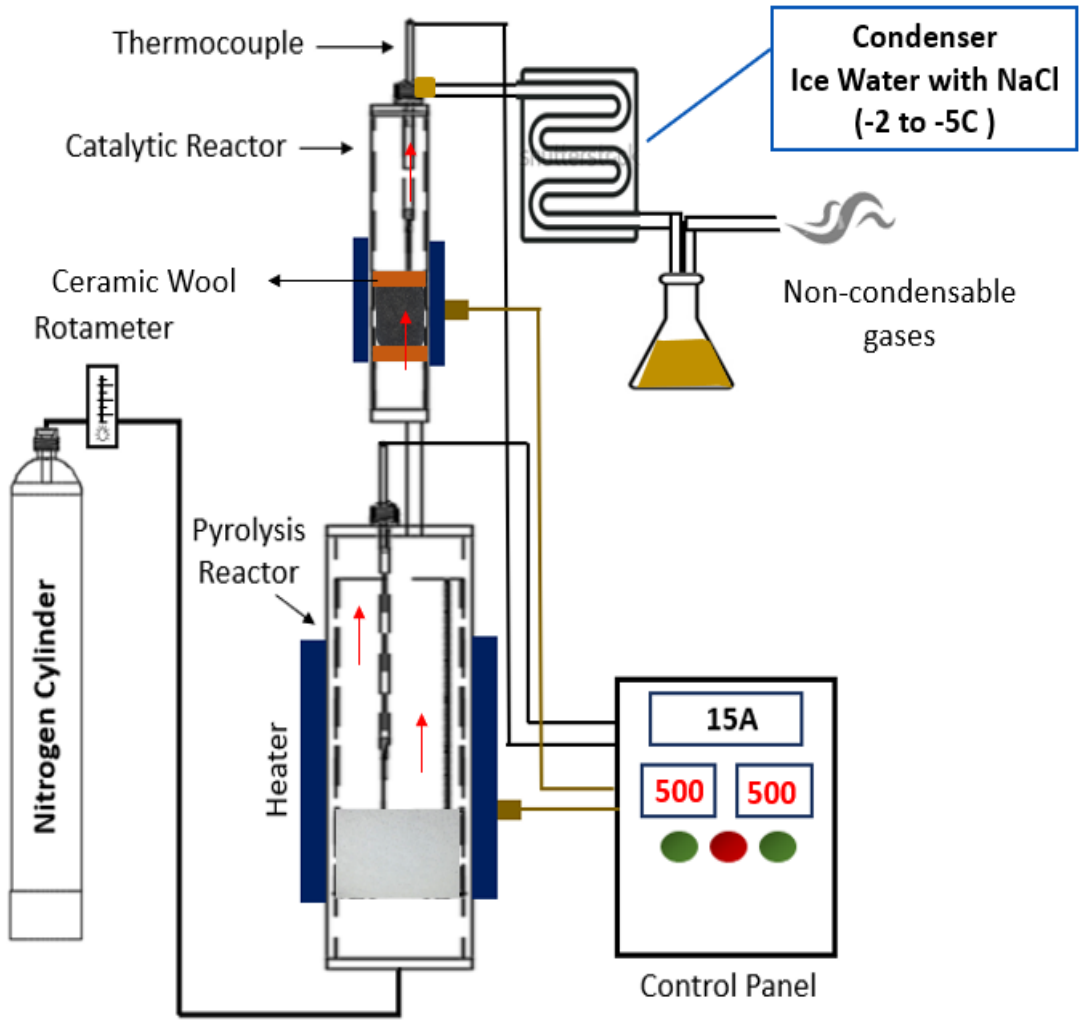

Figure 3.6 Schematic illustration of experimental setup

3.4.2 Experimental conditions

In each experiment, 60 g of feedstock was fed into R1 while 60 g sample of catalyst was used in R2 maintaining a catalyst to feedstock ratio (CFR) of 1 in catalytic experiments. Inert glass beads were used in R2 during non-catalytic experiments to ensure parallel operating conditions, such as mass and heat flow, as that of catalytic experimental runs. At first, the temperature of R2 was raised to 500°C and then the temperature of R1 was increased from room temperature to predetermined temperature of 500°C. Pyrolysis experiments were conducted until no more condensable vapours were observed in oil collecting flask. The oil fraction was computed by deducting the mass of flask and oil from the mass of empty flask (equation 1). Thereafter, pyrolytic oil was stored in the refrigerator to avoid the aging reactions. The solid residue i.e., char was collected from R1 and weighed. The yield of gas was evaluated by subtracting the weight of pyrolytic oil and char from the total weight of feedstock (equation 2). Coke deposition of catalyst was calculated by computing the difference in mass of original and spent catalyst (equation 3). Triplicates of each experiment were carried out and the average values have been reported.

$$\text{Oil yield} = \text{mass of flask and oil} - \text{mass of empty flask} \quad (1)$$

$$\text{Gas yield} = \text{Total mass of feedstock} - \text{mass of oil and char} \quad (2)$$

$$\text{Coke deposition} = \text{mass of spent catalyst} - \text{mass of original catalyst} \quad (3)$$

3.4.3 Pyrolytic Oil Phase Separation

Pyrolytic oil collected from catalytic and non-catalytic pyrolysis of feedstock consisted of two phases such as OP and AP, that were separated by giving retention time of 2

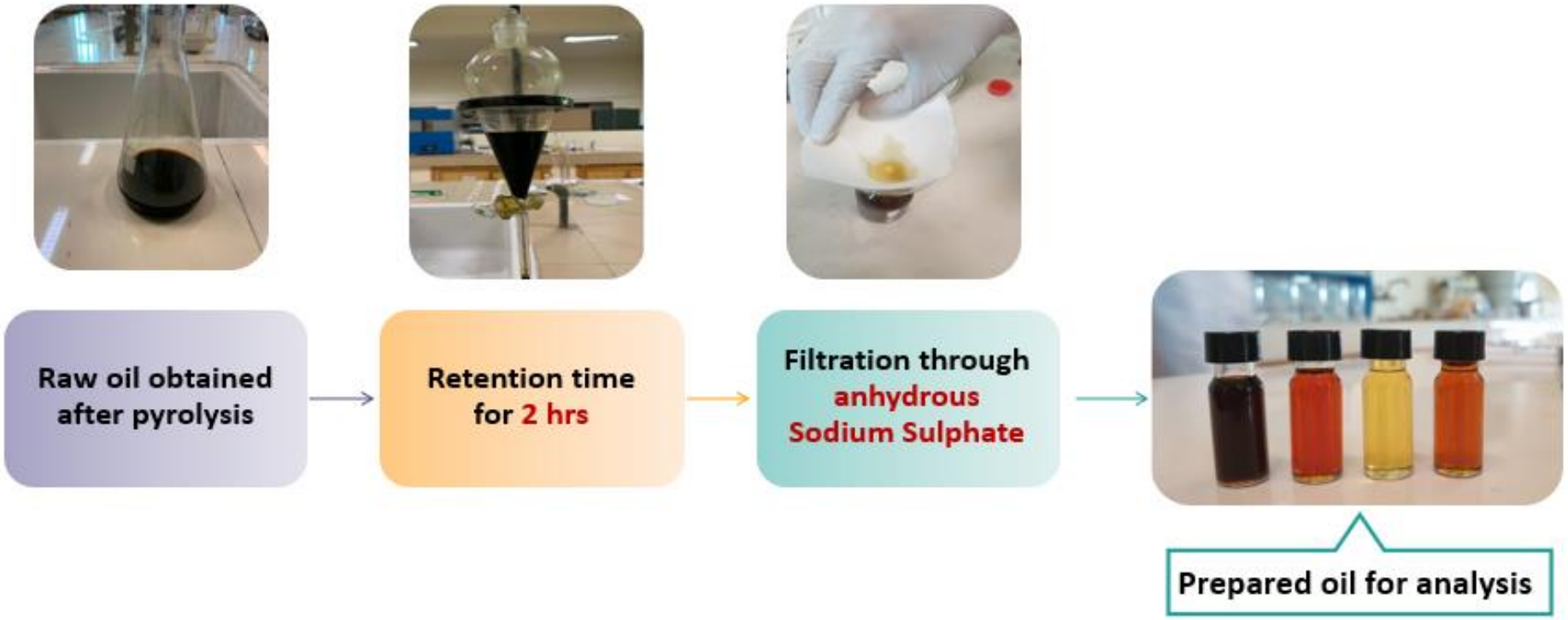

Figure 3.7 Pyrolytic oil processing

hours in separating funnel. The OP was filtered through a bed of anhydrous sodium sulphate to make it moisture free. The processing of pyrolytic oil to make the oil ready for analysis, is shown in figure

3.5 Pyrolytic Oil Characterization

Details of characterizations of chemical and physico chemical analysis of liquid oil obtained from the thermal and catalytic pyrolysis of polystyrene has been explained in the following headings.

3.5.1 Chemical Analysis

The chemical compounds in the liquid product were analysed by gas chromatography mass spectrometry GCMS (QP/2020 Schimadzu corporation) in conjunction with Schimadzu SH-Rxi-5Sil MS column having the dimensions of L = 30m, ID = 0.25mm and DF = 0.25mm. For column operation, helium gas was used as a carrier gas with the constant flowrate of 1mL/min whereas the sample of 1mL was injected at a split ratio of 80:1. Initially, the temperature of column was set at 30 °C and held for 1 min at and then programmed to increase to 290 °C with the heating rate of 8 °C / min where it was held for 2 min. Moreover, Trichloromethane solvent was used for dilution of oil sample to an appropriate concentration. After analysis, the spectra of chemical compounds were compared with the standard spectra in NIST library and literature.

3.5.2 Physicochemical Analysis

Physicochemical properties of pyrolytic oil specifically, HHV were calibrated using the instrument Isoperibol oxygen bomb calorimeter in accordance with the standard method ASTM D5861-1. Density of pyro oil was measured according to standard methods ASTM D4052. Flash point and viscosity of liquid was determined by Setaflash Series 3 Flash Point Tester and Redwood Viscometer respectively.

CHAPTER 4

4. RESULTS AND DISCUSSIONS

4.1 Raw Material and Feedstock Analysis

Different analysis of raw material i.e., CS and feedstock i.e., PS has been explained below in detail.

4.1.1 Physicochemical Analysis

Elemental analysis, proximate analysis, and HHV of CS and PS have been illustrated in table 4.1. CS is a potential source of carbon and contains 22.77 wt. % of fixed carbon (FC), 69.03 wt. % of volatile matter (VM) and 1.2 wt. % ash content. The percentage of ash content indicates that CS has less inorganic and lignin content as compared to cellulose content which is likely to produce catalysts with high porosity (Jayakumar, Zhao et al. 2018). The FC content of 22.77 wt. % in CS shows its potential to generate carbon products such as biochar and activated carbon (Dhyani and Bhaskar 2018). Similarly, lower ash content of CS is beneficial as high ash content in biochar/catalyst promotes undesired reactions and rupture of pore structure. The proximate analysis of PS revealed that it contains 99.7% volatiles which would result in maximum pyrolytic oil yield (Razzaq, Zeeshan et al. 2019). However, FC, ash content and moisture content (MC) were observed to be negligible in PS. The ultimate analysis of PS revealed it has high carbon content of 90.4 (wt.%) and hydrogen content of 8.57 (wt.%) which make it the most suitable candidate for pyrolysis (Oh, Lee et al. 2018).

Table 4.1 Feedstock and raw material characterization

	Proximate Analysis (wt.%)				Ultimate Analysis (wt.%)				HHV (MJ/kg)
	MC	**VM**	**Ash**	**FC**	**C**	**H**	**N**	**O**	
CS	7	69.03	1.2	22.77	52.03	18.04	0.43	29.5	18.5
PS	-	99.7	0.3	0	90.4	8.57	0.4	0.63	41

4.1.2 Thermogravimetric Analysis

TGA and DTGA curves of both CS and PS are presented in figures 4.1 and 4.2 respectively. It can be observed that thermal decomposition of raw material CS has been characterized by three stages due to three major components of biomass The mass loss (8.5%) of CS in first stage represents moisture loss which started at 100 °C. After the moisture loss, the remaining material in the coconut shell seemed to be thermally stable up to almost 200 °C. The sharp bend in the thermogram of CS occurred within the range of 250 °C – 390 °C and revealed the maximum loss of 63.87% which may be due to the loss of VM present. Second peak of DTG of CS indicates the contribution from pyrolysis of lignin and hemicellulose along with the cellulose pyrolysis. Similar trends have been noted by Yang et al., who evaluated that 93.5% of the pure cellulose pyrolyzed between 315 °C – 400 °C (Yang, Yan et al. 2007). Also, the rate of pyrolysis is maximum for hemicelluloses, cellulose, and lignin at the temperatures of 281°C, 339°C and 356°C respectively. Similar trends have been reported by researchers in the recent past (Liyanage and Pieris 2015).

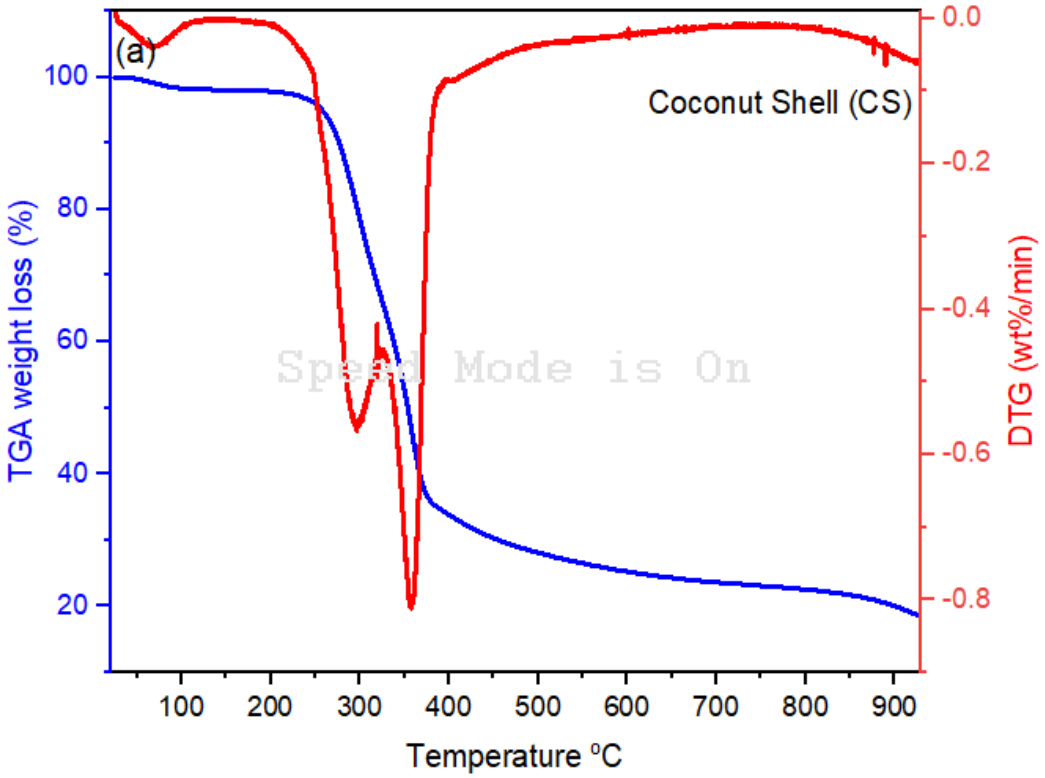

Figure 4.1 TG and DTG curve of Coconut Shell

On the other hand, PS thermogram indicated the negligible mass loss till 390°C which is mainly associated with its higher thermally stability due to long hydrocarbon chain and lower MC. However, the major mass loss of 99% was observed in the narrow temperature range of 390 °C - 500 °C which can be referred as the active pyrolytic zone of PS. It has been found that only 1 % of solid residue was left at a temperature of 500 °C which is in line with the results of pyrolysis experiments. The TGA results of PS are in consonance previous literature (Iftikhar, Zeeshan et al. 2019, Muneer, Zeeshan et al. 2019). The decomposition of PS above 500 °C is negligible which is represented by straight TGA and DTG curve of PS and therefore, 500 °C has been selected as the suitable temperature for its catalytic and non-catalytic pyrolysis.

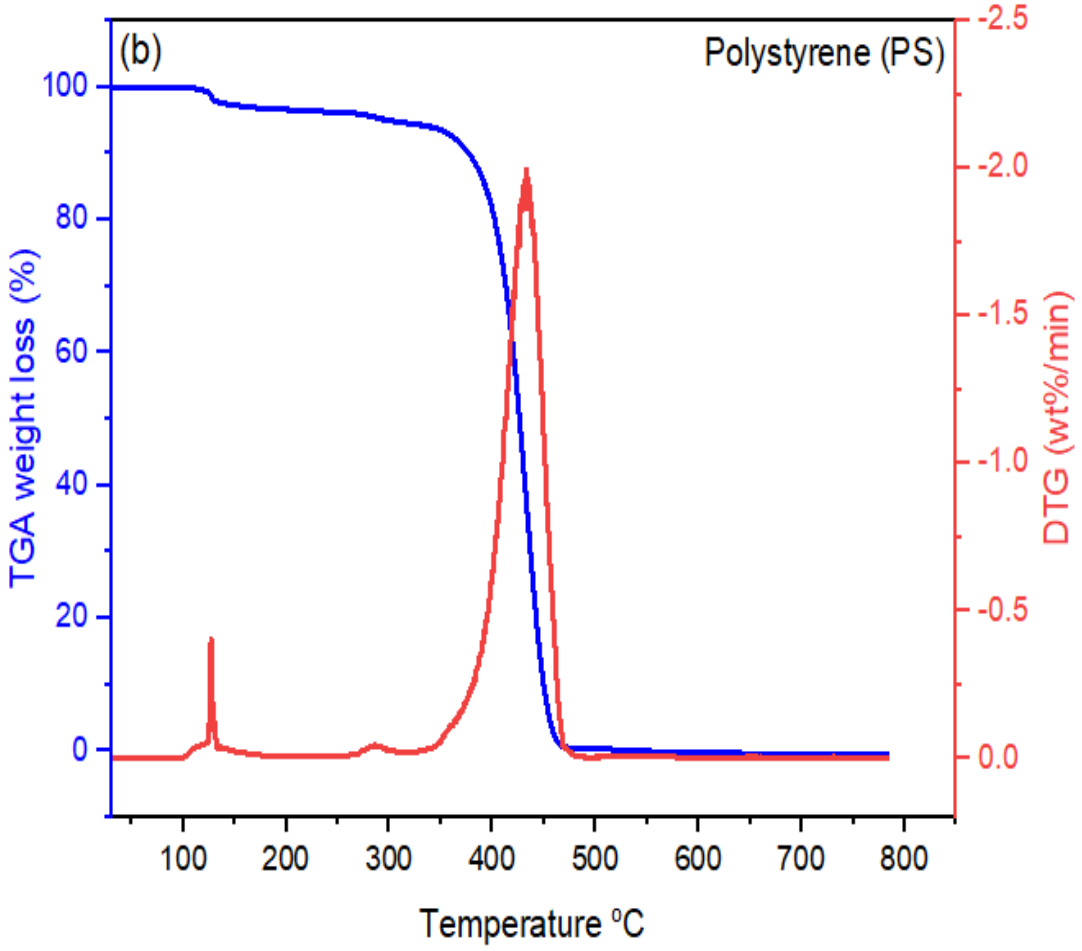

Figure 4.2 DTG and TG curve of Polystyrene

4.2 Catalysts Analysis

Chemical analysis, physicochemical analysis, textural properties and surface morphologies od catalysts used in the catalytic pyrolysis of PS have been mentioned in detail in the following sub sections.

4.2.1 Physicochemical Analysis

Table 4.2 represents the ultimate, proximate, and HHV of the catalysts. The elemental carbon in CSBC was 79.24 and increased to 84.31 in case of SAC and according to literature (Rex, Masilamani et al. 2020). The HHV of SAC is observed to decrease

comparatively as compared to CSBC due to formation of pores and cavities after thermal and chemical treatment.

Table 4.2 Physico-chemical properties of catalysts

	CSBC	**AC**	**CAC**
Proximate Analysis (wt.%)			
MC	3.25	2.12	2.46
VM	17.21	9.56	9.12
FC	76.6	83.12	82.62
Ash	2.94	5.2	5.8
Ultimate Analysis (wt.%)			
C	79.24	84.31	85.21
H	5.92	0	0
N	3.39	10.15	9.23
O	11.45	5.54	5.56
HHV (MJ/kg)	36	29	25

4.2.2 Textural properties

The effect of the thermal and chemical treatment on the BET surface area, pore volume and average pore diameter of catalysts are presented in table 4.3. It is conspicuous that BET surface area of AC has been improved compared to CSBC. Moreover, the average pore diameter of SAC was also increased many folds along with increased porosity due to activation. The increase in porosity and pore diameter, with chemical activation followed by thermal treatment, can be associated with release of tars / volatiles from

the cross-linked framework due higher temperature and impacts of acid. Similar observations have been reported by the previous literature (Yakout and El-Deen 2016).

Table 4.3 Textural properties of catalysts

	Surface area, m^2/g	**Pore volume, cm^3/g**	**Average pore diameter, nm**
CSBC	112	0.08	0.86
SAC	311	.0.31	31.84
CAC	805	0.27	31.98

4.2.3. XRD analysis

The X ray diffractogram of CSBC, SAC, and CAC is presented in figure 4.3. In this graph, the overall XRD profiles of three catalysts were found to be similar. The XRD profile of a CSBC produced at 600°C showed various broad peaks Which confirms its amorphous nature. The immediate broad peak is observed at an angle of 22° for biochar and it was further broadened into hump like pattern around 42°. This could be due to degradation of some of the components as biochar is synthesized higher temperature (Waqas, Aburiazaiza et al. 2018). Therefore, CS biochar didn't depict any sharp peak due to more amorphous nature and high surface area. In case of SAC, a diffraction peak at approximately 23.5° emerges that corresponded to crystal plane of activated carbon structure (Nizam, Hanafiah et al. 2021). Emergence of peaks at angles 22.8° and 29° indicate the formation of activated carbon. Moreover, a similar peak has also been observed for CAC at 26.6° which also confirms the formation of activated carbon.

.

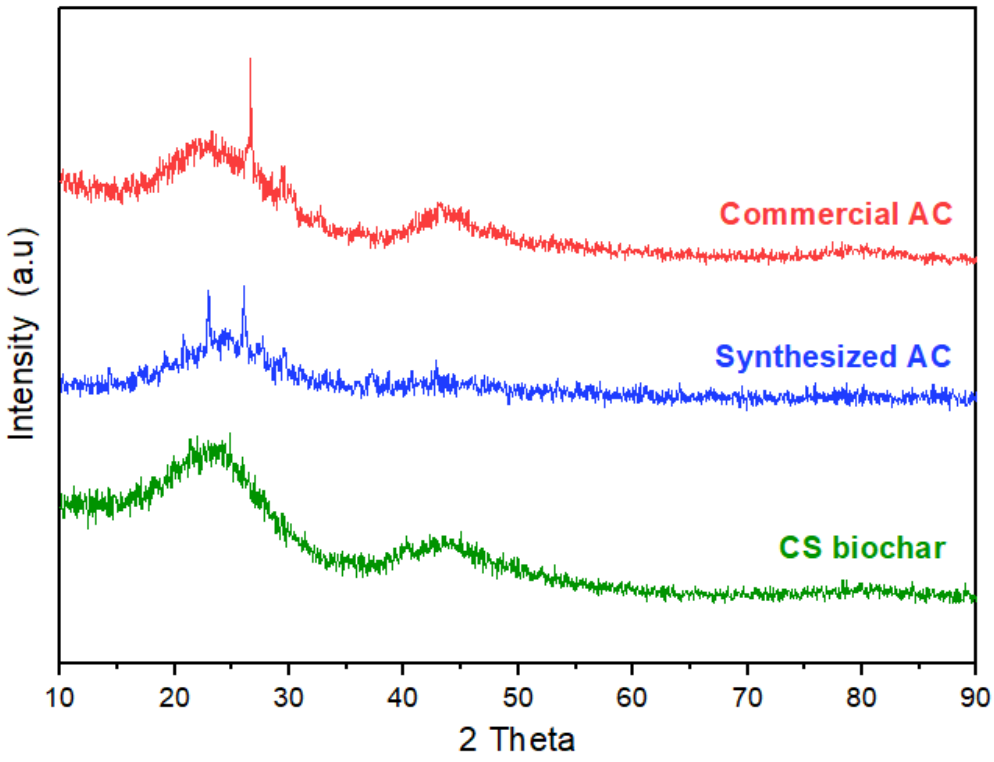

Figure 4.3 XRD patterns of CSBC, SAC and CAC

4.2.4 SEM analysis

SEM images of CS, CSBC, SAC and CAC at specific resolution of 10 µm and 20 kV voltage are given in figure 4.4. The change in surface morphology of all the samples can be noticed. CS exhibited sheet like structure as shown in figure 4.4 (a), however, disintegrated structure has been observed in case of CSBC which might be due to disruption of CS at high temperature during pyrolysis reactions. Furthermore, structure disintegration was intensified in case of SAC as shown in figure 4.4 (c) which might be associated with combined effect of impregnation of CSBC in H_3PO_4 and thermal treatment figure 4.4 (b and c). However, it is quite evident that no prominent pores have been observed on the surface of SAC. These observations correspond to the findings of previous literature (Prathiba, Shruthi et al. 2018).

(a) (b)

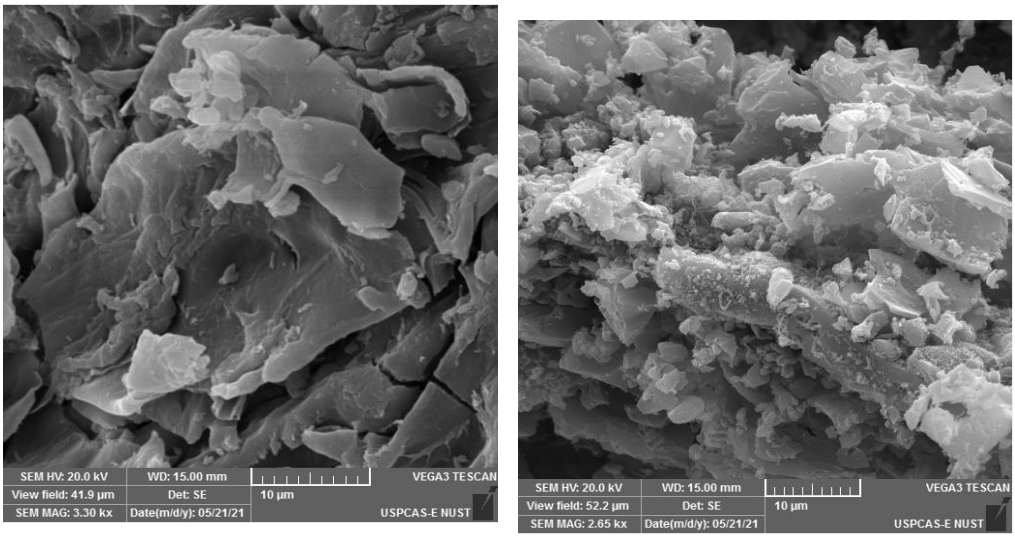

(c) (d)

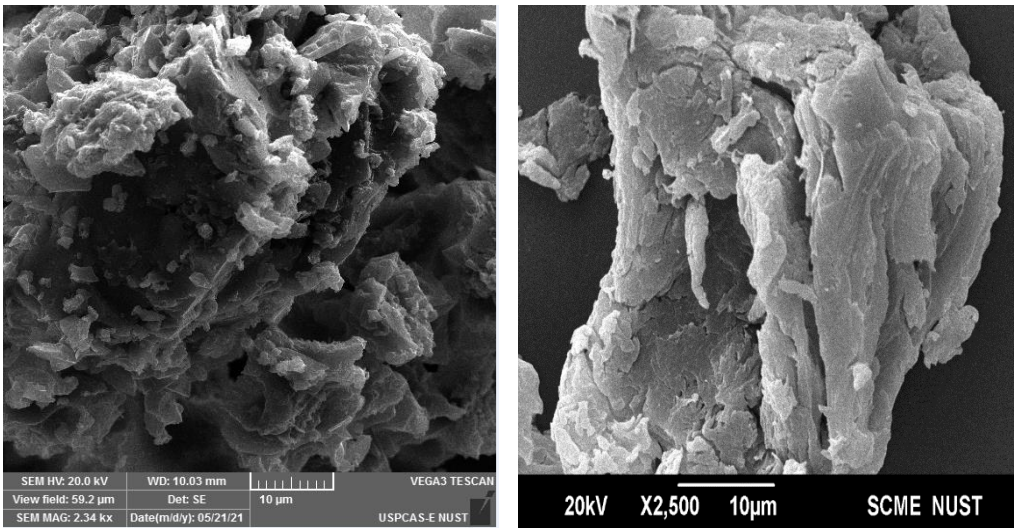

Figure 4.4 SEM photographs of (a) CS, (b) CSBC, (c) SAC and (d) CAC

4.2.5. Thermogravimetric analysis

Thermogravimetric analyses were conducted to determine the thermal degradation and stability of the catalysts. Figure 4.5 shows the thermograms of CSBC, SAC and CAC. In CSBC, weight loss of 1.38% was observed which indicates the moisture loss in CSBC. From 400 °C – 600 °C, uniform weight loss of 5.82% can be seen. The total weight loss of CSBC at 900 °C was observed to be 26.35%. Likewise,

in case of SAC, mass loss of 1.37% was observed at 100 °C that increased uniformly till 250 °C. Thereafter, at 650 °C mass loss of AC was 7.83% and the total mass loss of 15.6% had been seen in the range of 650 °C – 900 °C. The total mass loss of SAC at the final temperature of 900 °C was 22.22% which was less as compared to CSBC. Similarly, the thermogram of CAC revealed the mass loss of 2.33% at 100 °C The total mass loss reached to 50.97% at 900 °C which is highest among all three catalysts. Besides, the higher mass loss due to evaporation of moisture in the first phase indicates that CAC has relative higher affinity for moisture content compared to other as all the catalyst were preserved under same condition prior to TGA experiments. The observations suggests that SAC is most hydroscopic and stable catalyst among all. Carneiro, Lustosa Filho(Carneiro, Lustosa Filho et al. 2018) also reported that addition of chemicals in biochar increased the thermal stability as compared to raw biochar (Carneiro, Lustosa Filho et al. 2018).

4.2.6. FTIR analysis

FTIR spectrograms of CS, CSBC, SAC and CAC are represented in figure 4.6. Transmittance peaks corresponding to various frequencies have been compared with the relevant literature (Castilla-Caballero, Barraza-Burgos et al. 2020). In case of CS, a broad rounded peak can be seen in the region around 3400 cm^{-1} which confirms the presence of strong O-H stretching. The peak at 2926 cm^{-1} indicates presence of single carbon bonded to hydrogen C-H stretching. Similar peak is observed in CSBC and SAC as well. Sword like sharp peaks appeared around 1740 -1650 cm^{-1} attributed to the C=O groups. The stretching of C=C together with C=O stretching at 1611 cm^{-1} revealed the presence of aromatic compounds in CS. The sharp peak at 1031 cm^{-1} displayed the symmetric stretching of C-O-C bond which corresponds to aryl-alkyl ethers functional

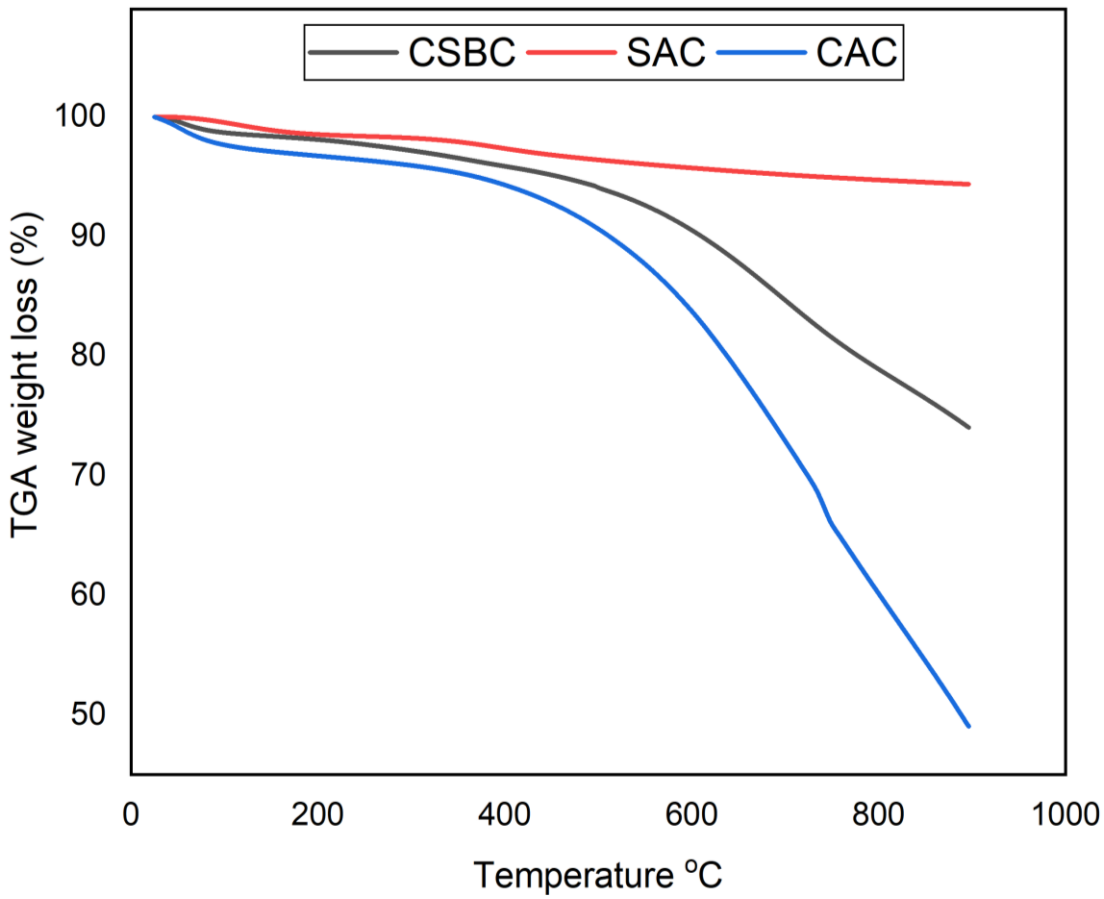

Figure 4.5 TGA curves of CSBC, SAC and CAC

groups present in cellulose, hemicellulose, and lignin. Various changes have been observed in the intensity of spectrograms in case of CSBC which are mainly associated with the release of volatiles from CS at temperature of 600 °C during pyrolysis reactions This might be due to the fact that biomass components (holocellulose and lignin) containing O-H functionality were decomposed during pyrolysis leading to removal of O-H which is indicated by the less intense peaks in CSBC compared to CS. Similarly, C-H stretches of medium intensity have been observed at 2926 cm^{-1}. Aromatic C-H bending appeared around 870 cm^{-1}. The prominent peak at 2582 and 607 cm^{-1} in CSBC is of carboxylic O-H stretching and triple bond alkyl carbon.

The presence of aromatic compounds in the SAC and CAC was confirmed by the medium stretching in the rings by the transmittance peak appeared at 1424 cm^{-1}. The

intensity of this peak is decreased in SAC due to chemical treatment with H_3PO_4. The band at 1037 cm^{-1} attributed to strong C-O stretch. The intensity of this band increased in SAC and CAC as compared to CSBC. In SAC slight peak was observed at 1228 cm^{-1} can be attributed to phosphate bonds in SAC which confirmed the presence of phosphate bonds in SAC (Zhang, Duan et al. 2019). The relative increase of this band in SAC suggests that these types of functional groups increased with the incorporation of chemicals and its subsequent thermal treatment at high temperature. Moreover, SAC and CAC displayed the small peak at 554 cm^{-1} depicts the presence of alkyl halides.

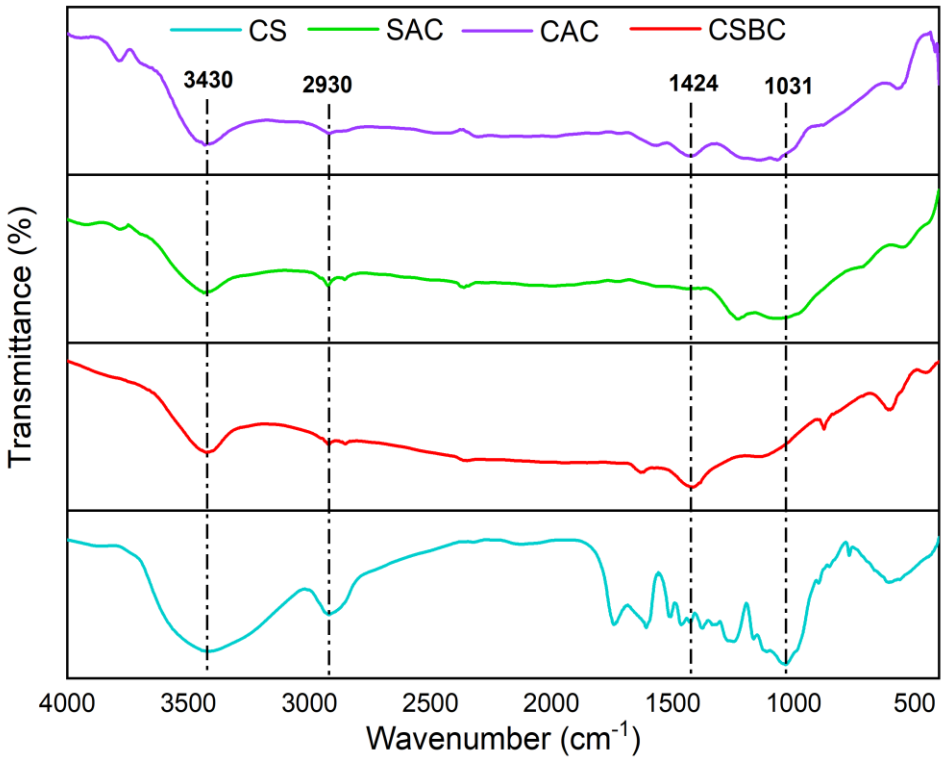

Figure 4.6 FTIR spectrum of CS, CSBC, SAC and CAC

4.3 Influence of catalysts on product distribution

The product yield of catalytic and non-catalytic pyrolysis products carried out at 500 °C has been presented in figure 4.7. It is clearly seen that the major product of PS pyrolysis is pyro oil followed by pyro gas as PS has 99.7% volatile as indicated by the proximate analysis (section 4.1.1). It should be noted that negligible solid residue has been observed in both thermal and catalytic pyrolysis which is in line with the TGA results. Moreover, maximum amount of oil has been observed in the non-catalytic pyrolysis of PS whereas gas yield was increased in the catalytic pyrolysis runs. In non-catalytic pyrolysis, higher pyro oil yield of 73 wt.% of has been observed. The incorporation of CSBC catalyst dramatically decreased the pyro-oil yield from 73 wt.% in case of non-catalytic pyrolysis of PS to 54 wt.% and enhanced the pyro gas yield from 26.1 wt.% to 44.1 wt.% in PS/CSBC combination. However, the pyro oil yield obtained from PS/SAC combination was 50 wt.% followed by gas yield of 47.6 wt.%. Whereas the pyro oil yield was slightly increased from 50 wt.% to 53 wt.% when steam activated CAC was employed as a catalyst. This indicates the depolymerization reactions were promoted in the presence of catalyst leading to production of non-condensable gas. Furthermore, the addition of catalyst enhanced the retention time of the volatiles in R2 which might also led to enhanced secondary reaction resulting in decreased oil yield and enhanced gaseous yield (Iftikhar, Zeeshan et al. 2019).

4.4. Influence of catalysts on composition of pyro oil

Chemical analysis such as gas chromatography mass spectrometry of catalytic pyrolytic oil obtained from catalytic pyrolysis of PS has been elaborated in the following sections.

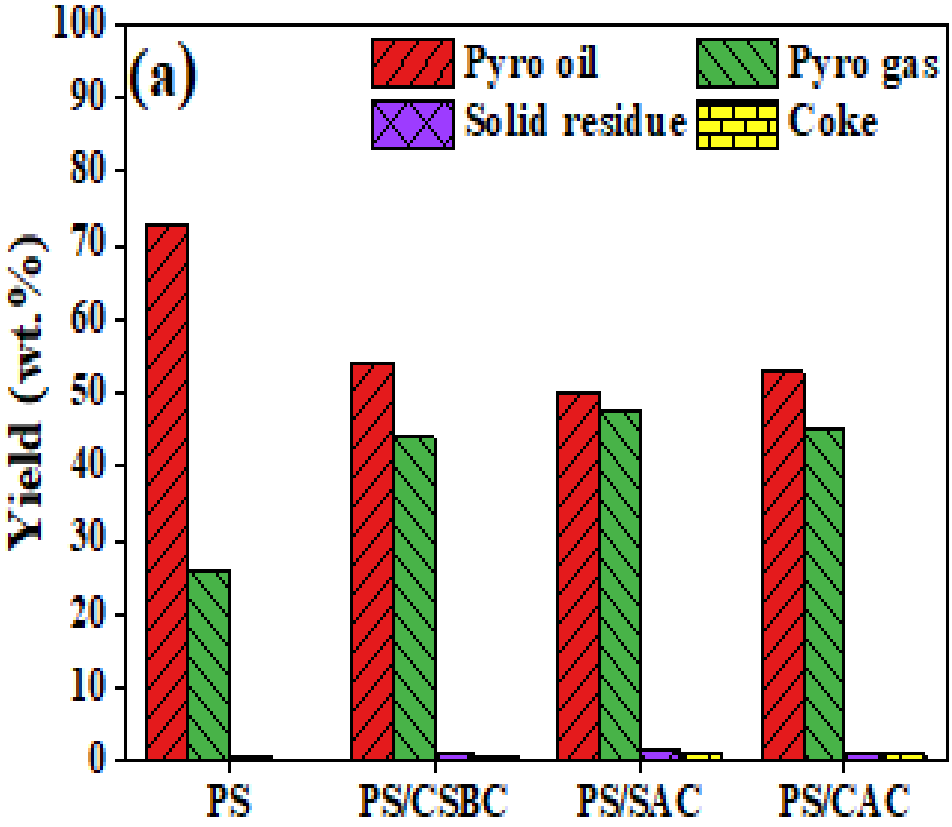

Figure 4.7 Product yields of pyrolysis products

4.4.1. Chemical analysis

To ensure brevity, the products of pyrolysis oil have been divided into three major categories including aromatics (MAHs and PAHs), aliphatic (Olefins and Paraffins) HCs, and unidentified compounds as shown in figure 4.8.

In non-catalytic pyrolysis of PS, 80.39 wt.% of MAHs were found. PS is an aromatic based feedstock and therefore its decomposition yielded higher amount aromatics and lower amount olefins (Rex, Masilamani et al. 2020). Among MAHs, styrene was the major compound with highest peak area % of 63 According to previous studies, the formation of styrene is associated with temperature range of 450-500 °C that increases its yield due to enhancement of polymer volatilization rate and end chain

β scission reactions of PS (Artetxe, Lopez et al. 2015). In addition to styrene, alpha methylstyrene and BTEX compounds were also produced from the decomposition of PS at this temperature. The total yield of PAHs was 6.24 wt.%.

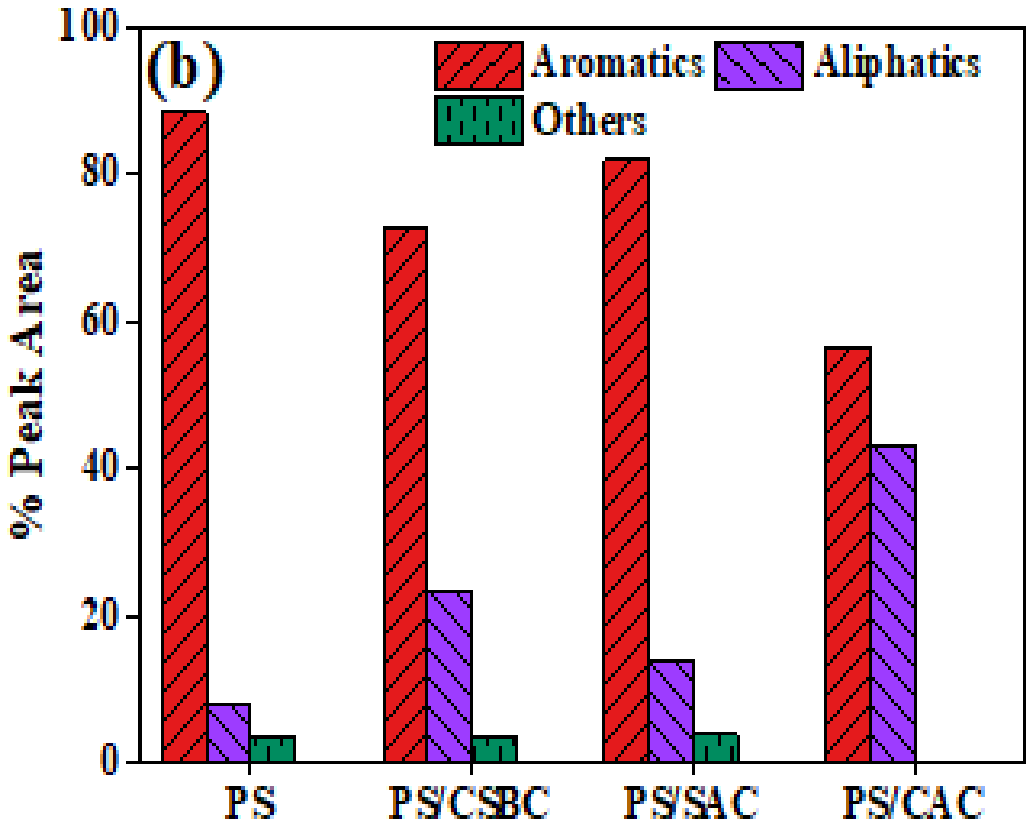

Figure 4.8 Percentage peak area of aromatics and aliphatic hydrocarbons

The incorporation of catalysts in PS significantly influenced the composition of pyro-oil. Addition of CSBC decreased the total aromatic and styrene content from 88.39 wt.% and 52.19 wt.% in case of thermal pyrolysis to 72.64 wt.% and 24 wt.% in case of CSBC however, the production of BTEX was enhanced from 17.8 wt.% to 29.6 wt.%. Moreover, the production of 23.6 wt.% was also observed with paraffins content of 11 peak area % and 12.6 peak area % of olefines. This can be explained by the fact that increased residence time due to incorporation of catalyst promoted the secondary

reactions and consequently depolymerization of PS leading to styrene yield suppression from 52.19 wt.% to 24 wt.% and enhancement of relatively lighter hydrocarbon fraction. It has been reported previously that coconut shell-based catalyst can potentially transform the polystyrene into simpler aromatics like BTEX instead of long polymer chains (Rex, Masilamani et al. 2020). It is also important to mention that PAHs yield was also increased from 8 wt.% to 13.64 wt.%. This might be associated with the repolymerization reactions of some MAHs compounds and formation of PAHs due to the catalyst reactivity and enhanced residence time (Muneer, Zeeshan et al. 2019). The aliphatic produced with addition of CSBC were in the range of C_8-C_{16} which is desired composition in Jet fuel. Several researchers have investigated the carbon-based catalysts to produced jet fuel however, the content of such hydrocarbons in present study was significantly lower compared to previous literature. Fan, Zhang studied the microwave assisted pyrolysis of polystyrene and found out that the pyro oil has the potential to be converted into aviation oil. The main components of the oils are in the range of jet fuel like hydrocarbons containing MAHs, PAHs and cycloalkenes with range of C_8-C_{16} (64.794–85.932 peak area%). The anomalies might be associated with different type of raw material of catalyst, pyrolysis feedstock, scale of experiment, type of reactor and operating conditions (Fan, Zhang et al. 2022).

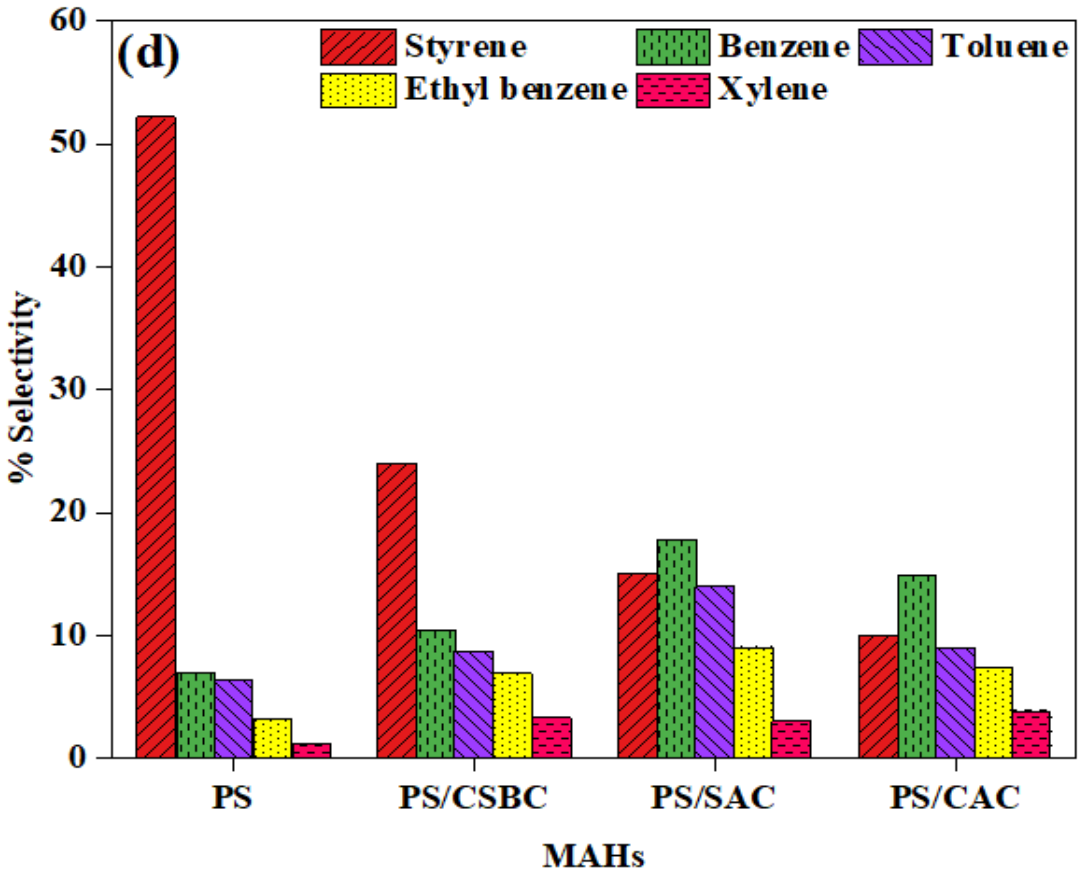

Figure 4.9 Percentage of selectivity of MAHs in pyro oil

The composition of pyro-oil was also affected with addition of SAC compared to pyrolysis of PS alone and PS/CSBC combination. The total aromatic content was lower than PS alone and higher than PS/CSBC combination (Fig. 6b) however, the BTEX selectivity was enhanced. The MAHs contributed about 65.7 wt.% of the total aromatic content. The increase in benzene content was highest which was followed by toluene and ethylbenzene. It is also to be mentioned that the aliphatic content was reduced as compared to PS/CSBC. It is speculated that transformation of aliphatic into BTEX was promoted in the presence of SAC. The enhancement in SAC selectivity for BTEX can be explained on the following grounds: The P containing functional group such as -O-P, O=P and -O-P-O were substituted on the surface and mesopores of the SAC during

chemical treatment with H_3PO_4. These functional group act as active acidic sites and promote the production of BTEX through aromatization reactions. Moreover, the surface area and carbon content of SAC was also higher compared to CSBC which might facilitate the transformation of aliphatic and styrene into BTEX. It has been reported previously that biomass derived activated carbon with P containing functional groups accelerate the aromatization reactions during the catalytic pyrolysis and produce aromatic hydrocarbons (Zhang, Lin et al. 2020, Duan, Feng et al. 2022). Also, the catalyst prepared by thermal treatment tend to have higher active sites that promote the production of aliphatic hydrocarbons particularly paraffins. The reduction of aliphatic hydrocarbons in SAC compared to CSBC could also be due to the difference in preparation method of two catalysts (Zhang, Duan et al. 2019). Moreover, the total PAHs content has also been increased to 16.3 wt.% in PS/SAC compared to both PS alone and PS/CSBC combination. Among PAHs, naphthalene and naphthalene, 2-phenyl- were dominating specie. This is due to increased acidic sites on SAC which promoted the cyclization of styrene monomers and repolymerisation reactions leading to formation of naphthalene and its compounds (Ding, Zhong et al. 2018). However, the production of PAHs remained lowered than that reported in previous literature who investigated the production of aromatics with various catalysts.

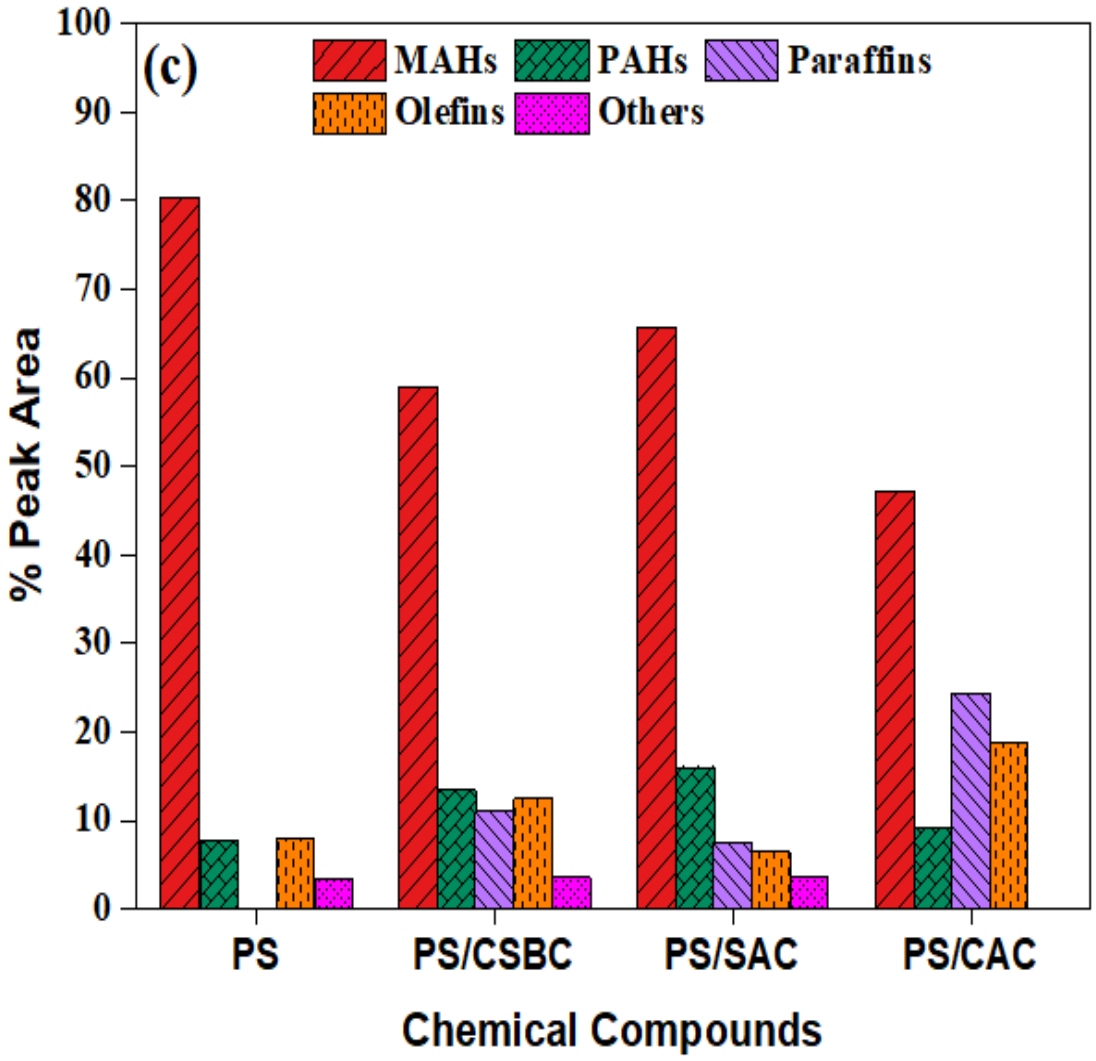

Figure 4.10 Peak percentage of chemical compounds in pyro oil

4.4.2 Comparison of synthetic activated carbon with commercial activated carbon.

The results of SAC were compared with steam activated CAC. Overall, the MAHs yield decreased from 65.70 wt.% in case SAC to 47.25 wt.% in the presence of CAC BTEX yield also has also been decreased from 44.2 wt.% observed in PS/SAC combination to 35.5 wt.% in case of PS/CAC combination. The reason for this is much higher surface area of CAC provides maximum catalytic sites for reaction which resulted in polymerisation of PS molecules. Moreover, the concentration of aliphatic hydrocarbons in case of PS/CAC was observed to be 43.37 wt.% which is higher as compared to 14

wt.% when SAC was employed as a catalyst. This could be linked to the steam activation of CAC. The steam activation has been reported to produce the types of functional groups on the surface that promote the C-C and C-H bond cracking resulting in the formation of relative light alkanes (Zhang, Duan et al. 2019). Additionally, the increased in light alkanes can be ascribed with the increased catalytic sites that favoured the C-C bond formation. On the other hand, the aromatization is caused by increased Bronsted acidic sites and subsequent dehydrogenation by the Lewis sites via a free radical mechanism within the activated carbon (Marcilla, Beltrán et al. 2009, Zhang, Duan et al. 2019).

4.4.3. Physicochemical analysis

Physicochemical properties of pyro oil have been enlisted in table 4.4. The flash point of all the fuels is lower than 30°C indicating that careful storage, handling, and utilization is required. Moreover, it was observed that the calorific value of oil increased from 41 to 46.14 MJ/kg with incorporation of catalysts. The value falls in the HHV range of conventional diesel and gasoline. The value of density of pyro oil varied from 0.73-0.89 which is in agreement with the previous literature. Similarly, the viscosity of pyro oil ranged between 0.73-0.89 cSt, which also comparable to that of gasoline. The lower viscosities are preferred for smooth running of engines (Khan and Zeeshan 2022).

Table 4.4 Physicochemical properties of pyro oil

	Pyrolytic oil				Conventional Fuels	
	PS	**PS/CSBC**	**PS/SAC**	**PS/CAC**	**Diesel**	**Gasoline**
HHV (MJ/kg)	41	43.44	45.26	46.14	42-45	42-46
Flash Point (°C)	<30	<30	<30	<30	53-80	-43
Viscosity at 40°C	1.66	1.92	1.89	1.41	2-5.5	1.17
Density at 20°C	0.89	0.79	0.75	0.73	0.81-0.87	0.72-0.78

CHAPTER 5

5. CONCLUSION AND RECOMMENDATIONS

5.1 Conclusion

The textural properties of CSBC were enhanced after treating it chemically and thermally. The chemical activation and thermal treatment increased the surface area, pore size, surface structure and carbon content of SAC. The highest oil yield of 73 wt.% was observed when the polystyrene was pyrolyzed in the absence of catalyst. However, the oil yield started decreasing with the addition of catalysts and the lowest oil yield of his 50 wt.% was observed when PS was pyrolyzed using SAC as a catalyst. Maximum styrene content was observed in non-catalytic pyrolysis whereas it decreased with the use of catalyst and lowest styrene content was observed in the presence of CSBC as a catalyst. While MAH content was increased in the presence of CSBC. The catalytic performance of SAC was superior to other catalysts in the terms of BTEX selectivity. Greater peak area % of 44.2 of MAH was calculated when PS was pyrolyzed using SAC. This could be due to improved surface characteristics of SAC that was a result of chemical and thermal activation. However, this was accompanied by PAHs content of 16.3 wt.%. The physicochemical characteristics of oil derived from PS/SAC were also improved compared to other combinations as calorific values comparable to gasoline were observed in the catalytic pyrolytic oils.

5.2 Recommendations

- Pre-treated biomass should be considered for the synthesis of AC.
- Reuse of BC and AC should be further studied.
- Other acids should be used for the chemical treatment of BC.
- Other plastics should be explored with coconut shell-based BC.

REFERENCES

1. Ahmad, M., A. U. Rajapaksha, J. E. Lim, M. Zhang, N. Bolan, D. Mohan, M. Vithanage, S. S. Lee and Y. S. J. C. Ok (2014). "Biochar as a sorbent for contaminant management in soil and water: a review." **99**: 19-33.

2. Cao, X., S. Sun and R. J. R. a. Sun (2017). "Application of biochar-based catalysts in biomass upgrading: a review." **7**(77): 48793-48805.

3. Castano, P., G. Elordi, M. Olazar, A. T. Aguayo, B. Pawelec and J. J. A. C. B. E. Bilbao (2011). "Insights into the coke deposited on HZSM-5, Hβ and HY zeolites during the cracking of polyethylene." **104**(1-2): 91-100.

4. Chi, N. T. L., S. Anto, T. S. Ahamed, S. S. Kumar, S. Shanmugam, M. S. Samuel, T. Mathimani, K. Brindhadevi and A. J. F. Pugazhendhi (2021). "A review on biochar production techniques and biochar based catalyst for biofuel production from algae." **287**: 119411.

5. Choudhary, T. K., K. S. Khan, Q. Hussain, M. Ahmad and M. J. A. J. o. G. Ashfaq (2019). "Feedstock-induced changes in composition and stability of biochar derived from different agricultural wastes." **12**(19): 1-13.

6. do Couto Fraga, A., C. P. B. Quitete, V. L. Ximenes, E. F. Sousa-Aguiar, I. M. Fonseca and A. M. B. J. J. o. M. C. A. C. Rego (2016). "Biomass derived solid acids as effective hydrolysis catalysts." **422**: 248-257.

7. Elordi, G., M. Olazar, G. Lopez, P. Castaño and J. J. A. C. B. E. Bilbao (2011). "Role of pore structure in the deactivation of zeolites (HZSM-5, Hβ and HY) by coke in the pyrolysis of polyethylene in a conical spouted bed reactor." **102**(1-2): 224-231.

8. Fechler, N., T. P. Fellinger and M. J. A. M. Antonietti (2013). "“Salt templating”: a simple and sustainable pathway toward highly porous functional carbons from ionic liquids." **25**(1): 75-79.

9. Foo, K. and B. J. B. T. Hameed (2012). "Mesoporous activated carbon from wood sawdust by K2CO3 activation using microwave heating." **111**: 425-432.

10. Gao, Y., Q. Yue, B. Gao and A. J. S. o. t. T. E. Li (2020). "Insight into activated carbon from different kinds of chemical activating agents: A review." **746**: 141094.

11. González-García, P. J. R. and S. E. Reviews (2018). "Activated carbon from lignocellulosics precursors: A review of the synthesis methods, characterization techniques and applications." **82**: 1393-1414.

12. Gupta, V., P. Carrott, R. Singh, M. Chaudhary and S. J. B. t. Kushwaha (2016). "Cellulose: a review as natural, modified and activated carbon adsorbent." **216**: 1066-1076.

13. Hu, X. and M. J. J. o. E. C. Gholizadeh (2019). "Biomass pyrolysis: A review of the process development and challenges from initial researches up to the commercialisation stage." **39**: 109-143.

14. Iwanow, M., J. Finkelmeyer, A. Söldner, M. Kaiser, T. Gärtner, V. Sieber and B. J. C. A. E. J. König (2017). "Preparation of supported palladium catalysts using deep eutectic solvents." **23**(51): 12467-12470.

15. Iwanow, M., T. Gärtner, V. Sieber and B. J. B. J. o. O. C. König (2020). "Activated carbon as catalyst support: precursors, preparation, modification and characterization." **16**(1): 1188-1202.

16. Jien, S.-H. (2019). Physical characteristics of biochars and their effects on soil physical properties. Biochar from Biomass and Waste, Elsevier**:** 21-35.

17. Kalderis, D., S. Bethanis, P. Paraskeva and E. J. B. t. Diamadopoulos (2008). "Production of activated carbon from bagasse and rice husk by a single-stage chemical activation method at low retention times." **99**(15): 6809-6816.

18. Khan, S. R., M. Zeeshan, A. Ahmed and S. J. J. o. C. P. Saeed (2021). "Comparison of synthetic and low-cost natural zeolite for bio-oil focused pyrolysis of raw and pretreated biomass." **313**: 127760.

19. Khuong, D. A., H. N. Nguyen, T. J. B. Tsubota and Bioenergy (2021). "Activated carbon produced from bamboo and solid residue by CO2 activation utilized as CO2 adsorbents." **148**: 106039.

20. Kosheleva, R. I., A. C. Mitropoulos and G. Z. J. E. C. L. Kyzas (2019). "Synthesis of activated carbon from food waste." **17**(1): 429-438.

21. Li, Y., L. Lu, S. Lyu, H. Xu, X. Ren, Y. A. J. J. o. A. Levendis and A. Pyrolysis (2021). "Activated coke preparation by physical activation of coal and biomass co-carbonized chars." **156**: 105137.

22. Lin, H.-T., M.-S. Huang, J.-W. Luo, L.-H. Lin, C.-M. Lee and K.-L. J. F. P. T. Ou (2010). "Hydrocarbon fuels produced by catalytic pyrolysis of hospital plastic wastes in a fluidizing cracking process." **91**(11): 1355-1363.

23. Liu, Y., M. Paskevicius, M. V. Sofianos, G. Parkinson, S. Wang and C.-Z. J. F. Li (2021). "A SAXS study of the pore structure evolution in biochar during gasification in H2O, CO2 and H2O/CO2." **292**: 120384.

24. Lopez, G., M. Artetxe, M. Amutio, J. Alvarez, J. Bilbao, M. J. R. Olazar and S. E. Reviews (2018). "Recent advances in the gasification of waste plastics. A critical overview." **82**: 576-596.

25. Lopez, G., M. Artetxe, M. Amutio, J. Bilbao, M. J. R. Olazar and S. E. Reviews (2017). "Thermochemical routes for the valorization of waste polyolefinic plastics to produce fuels and chemicals. A review." **73**: 346-368.

26. Lu, D., K. Yoshikawa, T. M. Ismail and M. J. A. e. Abd El-Salam (2018). "Assessment of the carbonized woody briquette gasification in an updraft fixed bed gasifier using the Euler-Euler model." **220**: 70-86.

27. Mazlan, M. A. F., Y. Uemura, S. Yusup, F. Elhassan, A. Uddin, A. Hiwada and M. J. P. e. Demiya (2016). "Activated carbon from rubber wood sawdust by carbon dioxide activation." **148**: 530-537.

28. Miskolczi, N., A. Angyal, L. Bartha and I. J. F. P. T. Valkai (2009). "Fuels by pyrolysis of waste plastics from agricultural and packaging sectors in a pilot scale reactor." **90**(7-8): 1032-1040.

29. Mukherjee, A. and R. J. S. r. Lal (2014). "The biochar dilemma." **52**(3): 217-230.

30. Mukome, F. N., X. Zhang, L. C. Silva, J. Six, S. J. J. J. o. a. Parikh and f. chemistry (2013). "Use of chemical and physical characteristics to investigate trends in biochar feedstocks." **61**(9): 2196-2204.

31. Renzini, M. S., U. Sedran, L. B. J. J. o. A. Pierella and A. Pyrolysis (2009). "H-ZSM-11 and Zn-ZSM-11 zeolites and their applications in the catalytic transformation of LDPE." **86**(1): 215-220.

32. Román, S., J. González, C. González-García and F. J. F. P. T. Zamora (2008). "Control of pore development during CO2 and steam activation of olive stones." **89**(8): 715-720.

33. Syamsiro, M., H. Saptoadi, T. Norsujianto, P. Noviasri, S. Cheng, Z. Alimuddin and K. J. E. P. Yoshikawa (2014). "Fuel oil production from municipal plastic wastes in sequential pyrolysis and catalytic reforming reactors." **47**: 180-188.

34. Ugwu, E. I., J. C. J. E. m. Agunwamba and assessment (2020). "A review on the applicability of activated carbon derived from plant biomass in adsorption of chromium, copper, and zinc from industrial wastewater." **192**(4): 1-12.

35. Wijitkosum, S. and P. J. A. S. Jiwnok (2019). "Elemental composition of biochar obtained from agricultural waste for soil amendment and carbon sequestration." **9**(19): 3980.

36. Xu, H., J. Guo and K. S. J. A. M. Suslick (2012). "Porous carbon spheres from energetic carbon precursors using ultrasonic spray pyrolysis." **24**(45): 6028-6033.

37. Yahya, M. A., Z. Al-Qodah, C. Z. J. R. Ngah and S. E. Reviews (2015). "Agricultural bio-waste materials as potential sustainable precursors used for activated carbon production: A review." **46**: 218-235.

38. Yang, J., L. Yue, B. Lin, L. Wang, Y. Zhao, Y. Lin, K. Chang, H. DaCosta, X. J. E. Hu and Fuels (2017). "CO2 Adsorption of nitrogen-doped carbons prepared from nitric acid preoxidized petroleum coke." **31**(10): 11060-11068.

39. Yang, Z., H. Lei, Y. Zhang, K. Qian, E. Villota, M. Qian, G. Yadavalli and H. J. A. E. Sun (2018). "Production of renewable alkyl-phenols from catalytic

pyrolysis of Douglas fir sawdust over biomass-derived activated carbons." **220**: 426-436.

40. Zhang, S., M. S. Miran, A. Ikoma, K. Dokko and M. J. J. o. t. A. C. S. Watanabe (2014). "Protic ionic liquids and salts as versatile carbon precursors." **136**(5): 1690-1693.

41. Zhao, R., N. Coles, Z. Kong, J. J. S. Wu and T. Research (2015). "Effects of aged and fresh biochars on soil acidity under different incubation conditions." **146**: 133-138.

42. Zuo, S., W. Zhang, Y. Wang, H. J. I. Xia and E. C. Research (2020). "Low-cost preparation of high-surface-area nitrogen-containing activated carbons from biomass-based chars by ammonia activation." **59**(16): 7527-7537.

43. Artetxe, M., G. Lopez, M. Amutio, I. Barbarias, A. Arregi, R. Aguado, J. Bilbao and M. J. W. m. Olazar (2015). "Styrene recovery from polystyrene by flash pyrolysis in a conical spouted bed reactor." **45**: 126-133.

44. Carneiro, J. S. d. S., J. F. Lustosa Filho, B. r. O. Nardis, J. Ribeiro-Soares, Y. L. Zinn, L. n. C. A. J. A. S. C. Melo and Engineering (2018). "Carbon stability of engineered biochar-based phosphate fertilizers." **6**(11): 14203-14212.

45. Castilla-Caballero, D., J. Barraza-Burgos, S. Gunasekaran, A. Roa-Espinosa, J. Colina-Márquez, F. Machuca-Martínez, A. Hernández-Ramírez and S. J. D. i. b. Vázquez-Rodríguez (2020). "Experimental data on the production and characterization of biochars derived from coconut-shell wastes obtained from the Colombian Pacific Coast at low temperature pyrolysis." **28**: 104855.

46. Dhyani, V. and T. J. R. e. Bhaskar (2018). "A comprehensive review on the pyrolysis of lignocellulosic biomass." **129**: 695-716.

47. Ding, K., Z. Zhong, J. Wang, B. Zhang, L. Fan, S. Liu, Y. Wang, Y. Liu, D. Zhong and P. J. B. t. Chen (2018). "Improving hydrocarbon yield from catalytic fast co-pyrolysis of hemicellulose and plastic in the dual-catalyst bed of CaO and HZSM-5." **261**: 86-92.

48. Duan, D., Z. Feng, Y. Zhang, T. Zhou, Z. Xu, Q. Wang, Y. Zhao, C. Wang and R. J. W. M. Ruan (2022). "Corncob pyrolysis: Improvement in hydrocarbon group types distribution of bio oil from co-catalysis over HZSM-5 and activated carbon." **141**: 8-15.

49. Fan, S., Y. Zhang, T. Liu, W. Fu, B. J. J. o. A. Li and A. Pyrolysis (2022). "Microwave-assisted pyrolysis of polystyrene for aviation oil production." **162**: 105425.

50. Hu, X. and M. J. J. o. E. C. Gholizadeh (2019). "Biomass pyrolysis: A review of the process development and challenges from initial researches up to the commercialisation stage." **39**: 109-143.

51. Iftikhar, H., M. Zeeshan, S. Iqbal, B. Muneer and M. J. B. t. Razzaq (2019). "Co-pyrolysis of sugarcane bagasse and polystyrene with ex-situ catalytic bed of metal oxides/HZSM-5 with focus on liquid yield." **289**: 121647.

52. Jayakumar, A., J. Zhao and J. M. J. C. Lee (2018). "A Coconut Leaf Sheath Derived Graphitized N-Doped Carbon Network for High-Performance Supercapacitors." **5**(2): 284-291.

53. Khan, S. R. and M. J. E. Zeeshan (2022). "Catalytic potential of low-cost natural zeolite and influence of various pretreatments of biomass on pyro-oil up-gradation during co-pyrolysis with scrap rubber tires." **238**: 121820.

54. Liyanage, C. D. and M. J. P. C. Pieris (2015). "A physico-chemical analysis of coconut shell powder." **16**: 222-228.

55. Marcilla, A., M. Beltrán and R. J. A. C. B. E. Navarro (2009). "Thermal and catalytic pyrolysis of polyethylene over HZSM5 and HUSY zeolites in a batch reactor under dynamic conditions." **86**(1-2): 78-86.

56. Mateo, W., H. Lei, E. Villota, M. Qian, Y. Zhao, E. Huo, Q. Zhang, X. Lin, C. Wang and Z. J. B. t. Huang (2020). "Synthesis and characterization of sulfonated activated carbon as a catalyst for bio-jet fuel production from biomass and waste plastics." **297**: 122411.

57. Muneer, B., M. Zeeshan, S. Qaisar, M. Razzaq and H. J. J. o. C. P. Iftikhar (2019). "Influence of in-situ and ex-situ HZSM-5 catalyst on co-pyrolysis of corn stalk and polystyrene with a focus on liquid yield and quality." **237**: 117762.

58. Nizam, N. U. M., M. M. Hanafiah, E. Mahmoudi, A. A. Halim and A. W. J. S. R. Mohammad (2021). "The removal of anionic and cationic dyes from an aqueous solution using biomass-based activated carbon." **11**(1): 1-17.

59. Oh, D., H. W. Lee, Y.-M. Kim and Y.-K. J. E. P. Park (2018). "Catalytic pyrolysis of polystyrene and polyethylene terephthalate over Al-MSU-F." **144**: 111-117.

60. Prathiba, R., M. Shruthi and L. R. J. W. M. Miranda (2018). "Pyrolysis of polystyrene waste in the presence of activated carbon in conventional and microwave heating using modified thermocouple." **76**: 528-536.

61. Razzaq, M., M. Zeeshan, S. Qaisar, H. Iftikhar and B. J. F. Muneer (2019). "Investigating use of metal-modified HZSM-5 catalyst to upgrade liquid yield in co-pyrolysis of wheat straw and polystyrene." **257**: 116119.

62. Rex, P., I. P. Masilamani and L. R. J. J. o. t. E. I. Miranda (2020). "Microwave pyrolysis of polystyrene and polypropylene mixtures using different activated carbon from biomass." **93**(5): 1819-1832.

63. Sun, K., Q. Huang, X. Meng, Y. Chi, J. J. E. Yan and Fuels (2018). "Catalytic pyrolysis of waste polyethylene into aromatics by H3PO4-activated carbon." **32**(9): 9772-9781.

64. Tsang, D. C., J. Hu, M. Y. Liu, W. Zhang, K. C. Lai, I. J. W. Lo, Air, and S. Pollution (2007). "Activated carbon produced from waste wood pallets: adsorption of three classes of dyes." **184**(1): 141-155.

65. Waqas, M., A. Aburiazaiza, R. Miandad, M. Rehan, M. Barakat and A. J. J. o. c. p. Nizami (2018). "Development of biochar as fuel and catalyst in energy recovery technologies." **188**: 477-488.

66. Yakout, S. and G. S. J. A. j. o. c. El-Deen (2016). "Characterization of activated carbon prepared by phosphoric acid activation of olive stones." **9**: S1155-S1162.

67. Yang, H., R. Yan, H. Chen, D. H. Lee and C. J. F. Zheng (2007). "Characteristics of hemicellulose, cellulose and lignin pyrolysis." **86**(12-13): 1781-1788.

68. Zhang, D., X. Lin, Q. Zhang, X. Ren, W. Yu and H. J. E. Cai (2020). "Catalytic pyrolysis of wood-plastic composite waste over activated carbon catalyst for

aromatics production: Effect of preparation process of activated carbon." **212**: 118983.

69. Zhang, Y., D. Duan, H. Lei, E. Villota and R. J. A. E. Ruan (2019). "Jet fuel production from waste plastics via catalytic pyrolysis with activated carbons." **251**: 113337.

70. Banu, J. R., V. G. Sharmila, U. Ushani, V. Amudha and G. J. S. o. t. T. E. Kumar (2020). "Impervious and influence in the liquid fuel production from municipal plastic waste through thermo-chemical biomass conversion technologies-A review." **718**: 137287.

71. Celik, G., R. M. Kennedy, R. A. Hackler, M. Ferrandon, A. Tennakoon, S. Patnaik, A. M. LaPointe, S. C. Ammal, A. Heyden and F. A. J. A. c. s. Perras (2019). "Upcycling single-use polyethylene into high-quality liquid products." **5**(11): 1795-1803.

72. Jambeck, J. R., R. Geyer, C. Wilcox, T. R. Siegler, M. Perryman, A. Andrady, R. Narayan and K. L. J. S. Law (2015). "Plastic waste inputs from land into the ocean." **347**(6223): 768-771.

73. Kasar, P., D. Sharma and M. J. J. o. C. P. Ahmaruzzaman (2020). "Thermal and catalytic decomposition of waste plastics and its co-processing with petroleum residue through pyrolysis process." **265**: 121639.

74. Lee, K.-H. and D.-H. J. W. M. Shin (2007). "Characteristics of liquid product from the pyrolysis of waste plastic mixture at low and high temperatures: Influence of lapse time of reaction." **27**(2): 168-176.

75. Lee, K.-H. J. J. o. A. and A. Pyrolysis (2012). "Effects of the types of zeolites on catalytic upgrading of pyrolysis wax oil." **94**: 209-214.

76. Lopez-Urionabarrenechea, A., I. De Marco, B. Caballero, M. Laresgoiti, A. J. J. o. a. Adrados and a. pyrolysis (2012). "Catalytic stepwise pyrolysis of packaging plastic waste." **96**: 54-62.

77. López, A., I. De Marco, B. Caballero, M. Laresgoiti, A. Adrados and A. J. A. C. B. E. Aranzabal (2011). "Catalytic pyrolysis of plastic wastes with two different types of catalysts: ZSM-5 zeolite and Red Mud." **104**(3-4): 211-219.

78. Maneechakr, P. and S. J. A. o. Karnjanakom (2021). "Improving the bio-oil quality via effective pyrolysis/deoxygenation of palm kernel cake over a metal (Cu, Ni, or Fe)-doped carbon catalyst." **6**(30): 20006-20014.

79. Maqsood, T., J. Dai, Y. Zhang, M. Guang, B. J. J. o. A. Li and A. Pyrolysis (2021). "Pyrolysis of plastic species: A review of resources and products." **159**: 105295.

80. Miandad, R., M. Barakat, A. S. Aburiazaiza, M. Rehan, A. J. P. S. Nizami and E. Protection (2016). "Catalytic pyrolysis of plastic waste: A review." **102**: 822-838.

81. Miskolczi, N., A. Angyal, L. Bartha and I. J. F. P. T. Valkai (2009). "Fuels by pyrolysis of waste plastics from agricultural and packaging sectors in a pilot scale reactor." **90**(7-8): 1032-1040.

82. Siddiqui, M. N. and H. H. J. F. P. T. Redhwi (2009). "Pyrolysis of mixed plastics for the recovery of useful products." **90**(4): 545-552.

83. Yao, D. and C.-H. J. A. E. Wang (2020). "Pyrolysis and in-line catalytic decomposition of polypropylene to carbon nanomaterials and hydrogen over Fe-and Ni-based catalysts." **265**: 114819.

84. Zhao, X., M. Korey, K. Li, K. Copenhaver, H. Tekinalp, S. Celik, K. Kalaitzidou, R. Ruan, A. J. Ragauskas and S. J. C. E. J. Ozcan (2022). "Plastic waste upcycling toward a circular economy." **428**: 131928.

85. Murdock, H. E., D. Gibb, T. André, J. L. Sawin, A. Brown, L. Ranalder, U. Collier, C. Dent, B. Epp and C. Hareesh Kumar (2021). "Renewables 2021-Global status report."

86. Li, Y., B. Li, X. Zhang, L. Chen, Q. Zhang, T. Wang, L. J. E. c. Ma and management (2016). "Continuous pyrolysis and catalytic upgrading of corncob hydrolysis residue in the combined system of auger reactor and downstream fixed-bed reactor." **122**: 1-9.